NOTICE

The quality of this microfiche is heavily dependent upon the quality of the original thesis submitted for microfilming. Every effort has been made to ensure the highest quality of reproduction possible.

If pages are missing, contact the university which granted the degree.

Some pages may have indistinct print especially if the original pages were typed with a poor typewriter ribbon or if the university sent us a poor photocopy.

Previously copyrighted materials (journal articles, published tests, etc.) are not filmed.

Reproduction in full or in part of this film is governed by the Canadian Copyright Act, R.S.C. 1970, c. C-30. Please read the authorization forms which accompany this thesis.

THIS DISSERTATION HAS BEEN MICROFILMED EXACTLY AS RECEIVED

AVIS

La qualité de cette microfiche dépend grandement de la qualité de la thèse soumise au microfilmage. Nous avons tout fait pour assurer une qualité supérieure de reproduction.

S'il manque des pages, veuillez communiquer avec l'université qui a conféré le grade.

La qualité d'impression de certaines pages peut laisser à désirer, surtout si les pages originales ont été dactylographiées à l'aide d'un ruban usé ou si l'université nous a fait parvenir une photocopie de mauvaise qualité.

Les documents qui font déjà l'objet d'un droit d'auteur (articles de revue, examens publiés, etc.) ne sont pas microfilmés.

La reproduction, même partielle, de ce microfilm est soumise à la Loi canadienne sur le droit d'auteur, SRC 1970, c. C-30. Veuillez prendre connaissance des formules d'autorisation qui accompagnent cette thèse.

LA THÈSE A ÉTÉ MICROFILMÉE TELLE QUE NOUS L'AVONS REÇUE

EFFECT OF CAVITATION NUMBER AND SOURCE SIZE ON CAVITATION DAMAGE

Yelwal Ranganath

A Thesis

in

The Faculty

of

Engineering

Presented in Partial Fulfillment of the Requirements for the degree of Master of Engineering at Concordia University Montreal, Quebec, Canada

June, 1978

ABSTRACT

ABSTRACT

EFFECT OF CAVITATION NUMBER AND SOURCE SIZE ON CAVITATION DAMAGE

Yelwal Ranganath

This thesis presents the results of an experimental investigation carried out to analyse the effect of cavitation number and source size on cavitation damage using a rotating disk facility. Soft aluminum plates mounted in the wake of triangular cavitating sources served as test specimens. The triangular source shape was chosen to eliminate Reynolds number effects.

It is shown that for a wide range of cavitation numbers a critical source size exists for which erosion is maximum at a fixed velocity. The maximum erosion for different velocities occur in a narrow band of cavitation numbers. Studies were also made to evaluate the velocity exponent influencing the cavitation erosion. The velocity exponent for weight loss due to cavitation damage is found to have an approximate value of 5.95 at maximum erosion conditions.

ACKNOWLEDGEMENT

ACKNOWLEDGEMENT

The author thanks Dr. A.S. Ramamurthy and Mr. L. Carballada for suggesting the problem and for their guidance throughout the course of this investigation. Greatful thanks are also due to Dr. Bhaskaran for his help.

The assistance of Messrs. Louis Stankevicius, Danny Roy and the members of the Machine Shop staff is acknowledged with thanks.

TABLE OF CONTENTS

TABLE OF CONTENTS

LIST OF FIGURES

LIST OF FIGURES

LIST OF TABLES

LIST OF TABLES

NOMENCLATURE

NOMENCLATURE

b	source size (prism width)
B	breadth of the specimen
d	maximum depth of penetration (Mdp)
f	vortex shedding frequency
ℓ	length of the cavity
L	length of the specimen
n, n_1, n_2	velocity exponents
P	undisturbed pressure of the approaching ambient flow
P_V	vapour pressure
r	radial distance of the source from the disk centre
R	Reynolds number Vd/ν
S	Strouhal number fb/V
t	test duration
T	temperature of water
V_j	contracted jet velocity
V	undisturbed velocity of the approaching flow
V_ϕ	circumferential velocity of the disk
W	weight loss due to cavitation erosion
W_{max}	maximum weight loss due to cavitation erosion

θ	angular measurement
λ	non-dimensional cavity length ℓ/b
ν	kinematic viscosity of water
ρ	density of water
σ	cavitation number
$\overline{\sigma}$	modified cavitation number
Ω	angular velocity

CHAPTER I

INTRODUCTION

CHAPTER I

INTRODUCTION

When the pressure in a liquid system is reduced dynamically at constant temperature, vapour or gas and vapour filled bubbles or cavities are formed. The formation of these bubbles, their growth and their subsequent collapse in the region of higher pressure is termed cavitation.

Hydraulic primemovers, flow-measuring equipment, hydraulic structures including conduits, space vehicles and nuclear reactors are very often affected by cavitation. Cavitation is also important in ship propellers operating at high speeds.

When cavitation occurs, the flow pattern is modified. Hence, the hydrodynamics of the flow between the liquid and the boundary is altered. There will be a decrease in the power output and efficiency in the case of turbines , reduction in the head and efficiency in the case of pumps indicating the effective decrease in momentum transfer between the liquid and the rotor. Besides, an increase in the resistance to flow of the liquid is also noticed [13].

Damage due to cavitation causes the removal of the material from the guiding surface. Other effects of cavitation which do not influence the flow or damage to the surfaces, but are otherwise relevant, are noise and vibration.

However, vibration leads to system instabilities.

Cavitation is undesirable, often destructive, except in the field of ocean surveys, the destruction of bacteria, emulsification techniques and depolymerisation.

Cavitation is mainly influenced by the properties of the liquid, geometry of the guiding surface, the turbulence and the boundary layer, amount of nuclei content in the liquid and the tensile strength of the liquid.

Laboratory studies have been conducted in order to determine the effects of cavitation [table 1]. However, in all these cases, cavitation is made to occur at specified locations. Being a high speed phenomenon, cavitation usually occurs at inaccssible places where direct observations cannot be made. Equipment generally used to study the various effects of cavitation are discussed in the fallowing paragraphs.

1) <u>Flow Apparatus</u>

Cavitation is produced on objects moved at high speeds through a liquid such as a rotating disk or a towing tank. Constricted passages such as venturies and nozzles are also included in this category.

2) <u>Acoustic Field Generators</u>

An electric field of sufficient intensity is applied across the conductive coating between the inner and outer surfaces of a barium titanate ring. The ring is placed below the free surface of a liquid contained in a glass cylinder. Large pressure is developed at the centre of the cylinder base due to the formation of a standing wave. Test specimens, if placed at this position, will be subjected to cavitation erosion.

3) Vibratory Methods

Test specimens are attached to a magnetostriction oscillator on the piezo-electric transducer devices; when vibration is produced, it gives rise to cavitation.

In the present investigation, a rotating disk facility is utilized. Cavitation is produced at a specified location under controlled pressure and temperature. The studies are carried out to find the velocity exponent for a wide range of cavitation numbers.

The weight loss of test specimens was measured for each test and the dependence of this weight on the velocity provided the velocity exponent. Thus,

$$V_1^{n_1}/V_2^{n_1} = (\Delta W_1)/(\Delta W_2) \qquad (1.1)$$

where

V_1 and V_2 = the velocities for two sets of conditions

ΔW_1 and ΔW_2 = the weight losses of the test specimen for velocities V_1 and V_2 (at fixed cavitation numbers.)

n_1 = the velocity exponent.

CHAPTER II

REVIEW OF THE EXISTING LITERATURE

CHAPTER II

REVIEW OF THE EXISTING LITERATURE

2.1 GENERAL REMARKS

Considerable data have been published on the hydrodynamic characteristics of flow-past cavitating sources [9,13,24,26] mounted in water tunnels, rotating disks and venturies. In most of the cases, two-dimensional cylinders were used as cavitating sources. Most of the test results obtained [16,18] were in the range of critical Reynolds number. Consequently, the test results were highly Reynolds number dependent.

Cylinders and triangular prisms are the most common types of two-dimensional cavitating sources. In the case of two-dimensional triangular prisms, Reynolds number is eliminated as a primary parameter since the separation points are fixed.

2.2 CAVITATION EROSION

Velocity dependence on cavitation erosion has been established by many investigators [9,12,16,21,24]. Studies conducted to find the relation between the erosion and the velocity showed that the damage due to cavitation is an exponential of the velocity. Based on weight or volume loss, it was established that

$$\text{weight or volume loss} = K_1 V^{n_1} \quad (2.1)$$

$$\text{weight or volume loss} = K_2 (V - V_0)^{n_2} \quad (2.2)$$

where

K_1 and K_2 are constants.

V = the velocity of flow.

V_0 = the velocity at which measurable cavitation erosion does not exist

n_1 and n_2 = the velocity exponents.

The investigations conducted by Shalnev [16] indicated that the exponent varies between 4 and 8. However, Knapp [12,13] and Kerr [11] obtained the mean value for the velocity exponent as 6 which was in good agreement between the water tunnel tests and the field turbine tests.

For two-dimensional circular cylinders at maximum erosion conditions, the exponent was found to be the least and equal to 5 by Ilichev [10]. However, Rao et al [18] stated that the exponent attained a maximum value of 17. The disagreement may be due to the Reynolds number effect associated with two-dimensional cylindrical cavitating sources.

The tests on erosion studies conducted on rotating hydrofoils by Tiruvengadam [20] indicated that the size of the source and the cavitation number had influence on damage characteristics of erosion and the velocity exponent. The velocity exponent computed from the results of these tests were of the order of 6.

Table 1 shows the values of the velocity exponents obtained by various investigators. The calculations were based on the selected damage criterion which represents variations based on weight loss or volume loss or the number of pits per second per square inch.

Test duration is an important parameter influencing the velocity exponent. In fact, studies conducted by Hammit et al [8] established that the increase in test duration resulted in an increased value of the exponent. On the other hand, Woods' [25] experimental data indicated that the velocity exponent decreased with an increase in test duration. The contradiction might be due to the unsteady rate of erosion.

Cavitation number, σ, is defined as

$$\sigma = \frac{P - P_V}{\frac{1}{2}\rho V^2} \qquad (2.3)$$

where

P = pressure in the undisturbed approaching flow

P_V = vapour pressure

ρ = mass density

V = mean velocity of the undisturbed approaching flow.

The length of the cavity ℓ, is the length from the edge of the source to the point where the cavity collapses.

Considerable amount of work have been done to determine the relationship between the cavitation number and the cavity length for two-dimensional sources. The experiments carried out by Varga and Sebestyn [24] in a closed circuit hydrodynamic tunnel revealed a hyperbolic variation between cavity length and cavitation number. The cavity length increased as the cavitation number decreased. It was also noticed that there was a critical cavity length at which rate of erosion was maximum. For the case of circular prisms the cavity length was observed to be dependent upon Reynolds number [24].

Recent investigations [14] on the effect of source size and velocity on structural damage due to cavitation erosion, reveal that a critical source size exists for a given cavitation number at a fixed velocity.

In Chapter IV, the effect of source size on cavitation erosion, effect of cavitation number on erosion, the velocity exponent and the data obtained by Stroboscopic observations on cavity length are discussed.

2.3 SCOPE OF THE PRESENT INVESTIGATION

The present investigation aims at determining the following:

(1) The velocity exponent for maximum cavitation damage.

(2) The effect of cavitation number on the erosion at fixed velocities and varying source sizes.

CHAPTER III

EXPERIMENTAL SET-UP AND PROCEDURE

CHAPTER III

EXPERIMENTAL SET-UP AND PROCEDURE

3.1 ROTATING DISK FACILITY

The present investigation was carried out using a rotating disk facility shown in Figure 1. The apparatus consists of a circular disk 2 feet in diameter, attached to a horizontal shaft, coupled to an 100 Hp, 1,800 RPM motor. The disk was housed in a chamber. The temperature of water in the chamber was maintained constant by continuous supply of fresh tap water. Settling vanes mounted on either side of the disk enhanced the induced circulation of water.

An equilateral triangular source made of brass shown in fig.2 is adopted. Triangular shape of the source is preferred to avoid Reynolds number as primary parameter while interpreing the results. The source width varied from 0.5 to 2.0 in. The maximum size is limited to 2 in. in order to avoid excessive pressure gradient across its face.

Soft aluminium test specimens of grade 1100-F are fixed flush on the disk down-stream in the early wake formed due to cavitating source. The size of the specimen was 5.25 x 2.5 in (Figure 2).

The specimen and source were mounted on the disk at a known radius thus enabling the peripheral velocity of the wheel to be obtained. The angular velocity of the disk is measured by a tachometer.

3.2 EXPERIMENTAL PROCEDURE

Tests were conducted at different cavitation numbers by choosing the chamber pressure and the velocity. Although one would like to cover a wide range of cavitation numbers in order to study their effect on the maximum damage (at fixed velocities), certain experimental limitations were encountered. For instance, the source size had to be increased with increasing cavitation numbers (see analysis of the results, page 14) at fixed velocities. When the width of the source was more than 2 inches, the damage proper tended to occur outside the test specimen. Consequently, the maximum size of the source was limited to 2 inches and hence the upper cavitation number was limited to 0.317. At very low ambient pressures, air entered the test chamber and hence the lower limit of cavitation number was set at 0.143 to eliminate errors due to the entry of air into the chamber.

For each test, new specimens were mounted with selected source sizes at fixed cavitation numbers. After each test, the specimens were cleaned, dried in a dessicator and weighed on a precision electronic balance to an accuracy of 0.1 mg. The cavity length was obtained with the help of a stroboscope used for visual observation.

The duration corresponding to the threshold value of damage was 9minutes. The duration of the test was selected to be much longer than the duration corresponding to the threshold value (figure 3). Also, preliminary tests conducted to study the effect of test duration on damage showed that a through hole was formed in the region, if the test duration were longer than 40 minutes in a few cases. As such a test duration of 30 minutes was chosen.

3.3 SURFACE PROFILE CHARACTERISTICS OF TEST SPECIMEN

The surface profile characteristics of the soft aluminium specimen before the test was obtained with the help of a profile recording device which has the commercial name "Telysurf". This instrument can discriminate undulations up to 0.0004". Plate 1 shows the Telesurf and its assembly.

When the surface irregularities are large, the Telesurf cannot be used. Hence, the surface profile of the specimens in some cases (after the tests) were obtained with the help of a Micro-positioner (Plate 2). This device could register undulations up to 0.001" (See also Appendix III).

3.4 EXPERIMENTAL ERRORS

The various error ranges encountered in the observations are given in Appendix IV. The error involved in calculating the non-dimensional variable, σ, is computed from the consideration of errors involved in individual variables.

CHAPTER IV

ANALYSIS OF RESULTS

CHAPTER IV

ANALYSIS OF RESULTS

4.1 EFFECT OF SOURCE SIZE ON CAVITATION EROSION

In this section the variation of weight loss due to cavitation erosion on aluminium test specimen caused by triangular cavitating sources is discussed. The erosion is essentially in the early wake of cavitating body. The studies are carried out at fixed cavitation numbers (σ).

Figures 4 to 7 show the variation of weight loss with respect to the size of the source at constant cavitation numbers. Four narrow ranges of cavitation numbers and four different velocities were selected for each test series in which the weight loss was determined. The plots also show that the ratio of weight loss to maximum weight loss for a fixed range of cavitation number increases with an increase in source size, reaching a maximum (critical source size) and beyond this the weight loss decreases with further increase in source size.

Under controlled conditions (fixed velocities and cavitation number), a decrease in source size increases the frequency of pressure pulsations. Thus the damage is increased up to a certain source size. When the source size is extremely small, its effect is local and not much damage could be expected.

4.2 EFFECT OF VELOCITY

As one would expect, the maximum weight loss increases with increase in velocity. An increase in velocity registers an increase in the frequency of vortex shedding which, in turn, increases the pressure pulsation frequency in the source wake. As stated earlier, these pressure pulsations promote the damage potential at a given stress level. This inference agrees well with existing test results [3a,18], (and Table 1).

For maximum damage, an increase in the velocity appears to result in a reduced source size (Figs. 4 to 7).

4.3 EFFECT OF CAVITATION NUMBER ON EROSION AT FIXED VELOCITIES

Figure 8, obtained with the help of Figs. 4 to 7, shows the relation between the maximum erosion and the cavitation number at different velocities which form the group parameter. It is clear from Figure 8 that the maximum cavitation erosion occurs in the critical cavitation number range which is close to 0.257. This number is nearly the same for all the velocities covered.

When the cavitation number is decreased from its maximum value, the erosion increases, reaches a maximum value and then decreases. It has been observed that the cavitation bubbles move approximately at the same speed as the liquid [9].

Consider the situation in which the cavitation number is decreased by keeping the velocity constant and reducing the pressure. Since the length of the cavity increases with decrease in cavitation number, the time for bubble growth increases and hence the dominant bubble size will be relatively larger at lower cavitation numbers. Further, these larger cavitation bubbles can penetrate the high pressure region and their damage potential is higher. However, the reduction of the pressure to reduce the cavitation number will also reduce the collapse pressure of bubbles. In fact, very little damage occurs when the cavitation region entirely envelopes the test specimen. Consequently, the overall damage potential of the bubbles will increase to a maximum and then decrease due to the effect of the two opposing variables, namely the size of bubbles and the ambient pressure at which they collapse.

The range of cavitation numbers in which maximum damage occurs is the same.

In the present study maximum damage was observed to occur within a narrow band of cavitation numbers ($0.252 < \sigma < 0.257$). The dependence of erosion on cavitation number is very similar for all the velocities.

4.4 VELOCITY EXPONENT

Figure 9 shows a logarithmic plot between the velocity and weight loss at maximum erosion conditions for different ranges of cavitation numbers. For a given cavitation number range, the weight loss appears to be related by an equation of the following form:

$$\Delta W \;\alpha\; V^{n_1} \tag{4.1}$$

where

ΔW = the weight loss

V = the velocity,

and

n_1 = the exponent of velocity

The value of n_1 is essentially a constant for all the cavitation ranges selected. It is only at very low velocities that this relationship appear to break down. A few relevant remarks are made below.

Although the only velocity used for computation in Equation (2.3), is the circumferential velocity V_ϕ, the true relative velocity should also include the vector addition of radial and axial velocities to V_ϕ. Hence, at lower velocities these components must significantly influence the damage of the specimen. Further, the flow characteristics near the centre of the rotating disk are affected by the presence of elements such as fasteners used to fix the disk to the rotating shaft.

In the linear portion of the graph, its slope for all ranges of cavitation number is found to be nearly 5.95. This is in good agreement with the published data [3a,16].

4.5 CAVITATION NUMBER AND CAVITY LENGTH

Figure 14 shows the variation of the non-dimensional cavity length (λ) with the cavitation number (σ). It can be observed that an increase in the cavitation number decreases the cavity length for a given source size. A brief discussion on the characteristics of this graph is given in Appendix II.

4.6 DAMAGE CHARACTERISTICS OF THE TEST SPECIMEN

Figures 11 and 12 show typical surface profiles of the damaged specimens (RUN 262 and 128, Tables 4 and 5 The line OACB is obtained by joining the centre of the source (O) to the maximum depth of penetration (C). AB is the interval selected to draw the profiles (see also Appendix III).

Tables II to V give the variations of the maximum depth of penetration, Mdp, with respect to damage. It is observed that with an increase in damage, the Mdp will also be increased. The source also influences the Mdp in just the same way as it influences the erosion.

The variation of Mdp with cavitation number at peak erosion conditions is shown in Fig. 1 . For the set of velocities selected, the maximum depth of penetration occurs within a narrow band of cavitation numbers ($0.252 < \sigma < 0.257$).

CHAPTER V

CONCLUSIONS

CHAPTER V

CONCLUSIONS

5.1 CONCLUSIONS

(1) The present studies confirm the earlier prediction [3a] that the maximum cavitation damage occurs at a critical source size. In the present tests, a range of cavitation numbers were covered to study this behaviour. The data indicates that maximum damage is associated with a critical source size when the cavitation number and the velocity are held constant.

(2) The weight loss is a function of cavitation number at fixed velocities. The variation of weight loss with cavitation number is similar for all the selected velocities. At the velocities chosen, the maximum erosion appears to occur in a narrow band of cavitation numbers.

(3) At the maximum erosion conditions, the velocity exponent defined by n_1 in Equation (2.1) is found to be close to 5.95. Any increase in velocity will result in increased weight loss at maximum erosion conditions.

(4) The critical size of the source for each fixed velocity increases with an increase in cavitation number.

(5) The behaviour of the maximum depth of penetration with a cavitation number is similar to that of weight loss for fixed velocities.

5.2 SCOPE FOR FURTHER WORK

As a further extension of the present work one could study the effects of noise intensities on cavitation erosion. The effect of test duration on the velocity exponent can also be studied. Further, one can conduct a detailed investigation of the surface characteristics of the damaged specimen and try to relate it to the fluid dynamic parameters.

REFERENCES

REFERENCES

[1] Bearman, P.W., "On Vortex Shedding From a Circular Cylinder in Critical Reynolds Number Regime", J. Fluid Mechanics, Vol.37, 1969, pp.77-565.

[2] Benjamin, T.B., and Ellis, A.T., "The Collapse of Cavitation Bubbles and the Pressure Thereby Produced Against Solid Boundaries", Phil.Trans.Royal Soc., (London), Vol.A, No.260, 1966, pp.221-240.

[3a] Bhaskaran, P., "Characteristics of Flow Past Bluff Cavitating Sources", D.Engg.Thesis, Department of Civil Engineering, Concordia University, Montreal, Canada, 1978.

[3b] Birkhoff, G., Plesset, M. and Simmons, N., "Wall Effects in Cavity Flow", Part 1: Quarterly of Applied Mathematics, Vol.8, No. 2, 1950, pp.151-168; Part 2, Vol. 9, No. 4, 1952, pp.413-421.

[4] Canavelis, R., "Effects of Velocity and Static Pressure on Cavitation Damage", ASME, Cavitation Forum, 1968.

[5] Daily, J.W., and Harleman, D.R.F., Fluid Dynamics, Addison-Wesley Publishing Company.

[6] Ellis, A.T., Gruber, G., and George, N., "An Experimental Investigation of Short-Wave-Bubble Interaction and Reflection. Holograms of Long Polymer Molecules", California Institute of Technology, Div. of Engineering and Applied Science, Rep.E-115-A.1, 1968.

[7] Hammit, F.G., "Observation on Cavitation Damage in a Flowing System", Trans.ASME, Ser.D,85, Sept.1963, pp.347-359.

[8] Hammit, F.G., Barinka, L.L., Robinson,M.J., Pehlbe,R.D., and Siebert, C.A., "Initial Phases of Damage to Test Specimens in a Cavitating Venturi", Trans.ASME, Ser.D., 87, 1965, pp.453-464.

[9] Hammit, F.G., "Damage to Solids Caused by Cavitation", Royal Soc. London, Phil.Trans.A. 260, 1966, pp.245-255.

[10] Ilichev, V.I., and Kurietsov, G.N., "Relations Between Acoustic Noise and Erosion in Hydrodynamic Cavitation", Soviet Physics, Doklody 13,4, Oct.1968, pp.313-316.

[11] Kerr, S.K., and Rosenberg, K., "An Index of Cavitation Erosion by Means of Radioisotopes", Trans. ASME, 80,6,1958, pp.1045-1054.

[12] Knapp, R.T., "Recent Investigation of the Mechanics of Cavitation and Cavitation Damage", Trans.ASME, 77, Oct.1955, pp.1045-1054.

[13] Knapp, R.T., Daily, J.W., and Hammit, F.G., Cavitation, McGraw-Hill Book Co., 1970.

[14] Ramamurthy, A.S., Bhaskaran, P., "Source Size and Velocity Effects on Cavitation Damage", Trans.ASME, J. Fluids Eng. 97,3,1975,pp.384-386.

[15] Ramamurthy, A.S., Bhaskaran, P., and Subramanya,K., "Use of Wake Interference Element to Reduce Cavitation Damage", ASME Cavitation and Polyphase Flow Forum, 1974.

[16] Shalnev,K.K., "Experimental Study of the Intensity of Erosion Due to Cavitation", Proc.Symp. on Cavitation in Hydrodyn.NPL,1955.

[17] Shalnev, K.K., "Boundary Effects on Cavitating Plane Past a Cylinder", J.Applied Mechanics and Tech.Phys.No.3 (Zhurnal Prikladnoi Meckniki i Tecnichiskoi.Fiziki,No.3),1965, pp.103-108,pp.73-76.

[18] Syamala Rao, B.C., Lakshmana Rao, N.S., Seetharamiah, K., "Cavitation Erosion Studies With Venturi and Rotation Disk in Water", Trans.ASME D, 1970,pp.563-579.

[19] Syamala Rao, B.C., and Chandrashekara, D.V., "Some Characteristics of Cavity Flow Past Cylindrical Inducers in a Venturi", ASME Paper 75-WA/FE-7, 1975.

[20] Thiruvengadam, A., "A Unified Theory of Cavitation Damage", ASME, Paper No.62-wa-118,1962.

[21] Thiruvengadam, A., "Cavitation Erosion", Applied Mechanics Reviews, March 1971, pp.245-252.

[22] Thiruvengadam, A., "Scaling Laws for Cavitation Erosion", Tech.Rep. 233-15, Hydronautics, Dec.1971.

[23] Varga, J. "Einige Forschungsergebnisse auf dem Gebiete der Kavitationsstromung und der Kavitationserosion", Osterreichische Ingenieur-Zeitcehrift, August 1968, pp. 266-271.

[24] Varga,J. and Sebestyn,G.Y., "Determination of the Frequencies of Wakes Shedding From Circular Cylinders", Acta Technica 53, 1966, pp.91-108.

[25] Wood, G.M., Knudsen,L.K., and Hammit, F.G., "Cavitation Damage Studies With Rotating Disk in Water", Trans.ASME, 89,D,1,1967,pp.98-110.

[26] Younge,J.O., and Holl,J.W., "Effects of Cavitation on Periodic Wakes Behind Symmetric Wedges", J.Basic Engineering, Trans.ASME, March 1966, pp.163-176.

FIGURES

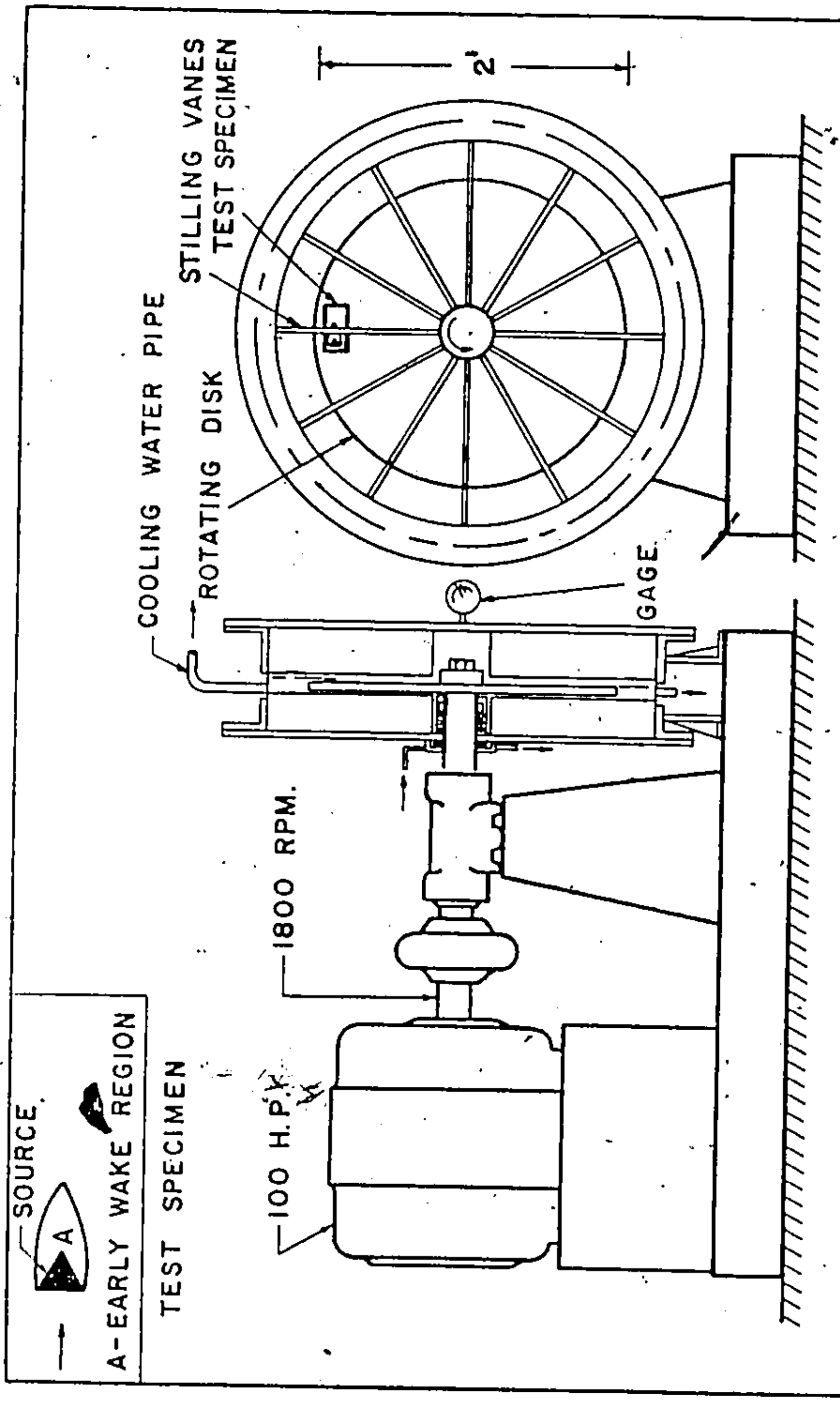

FIG. 1 ROTATING DISK FACILITY

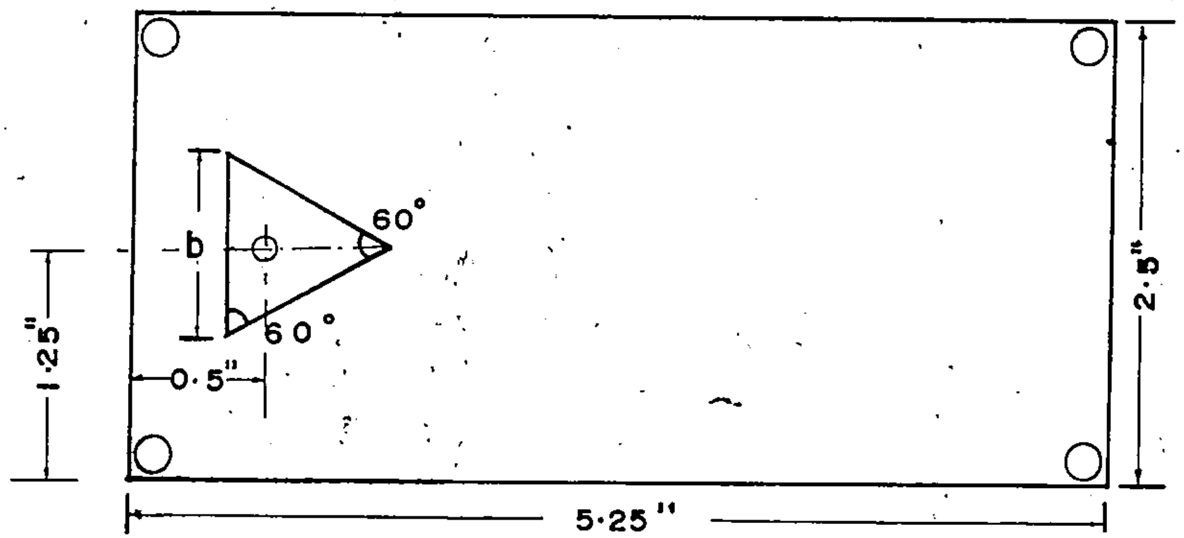

b (inches) 0·5, 0·75, 0·875, 1·0, 1·125, 1·25, 1·375,
1·5, 1·625, 1·75, 1·875, 1·925, 2·0

FIG. 2., CAVITATING SOURCE & TEST SPECIMEN

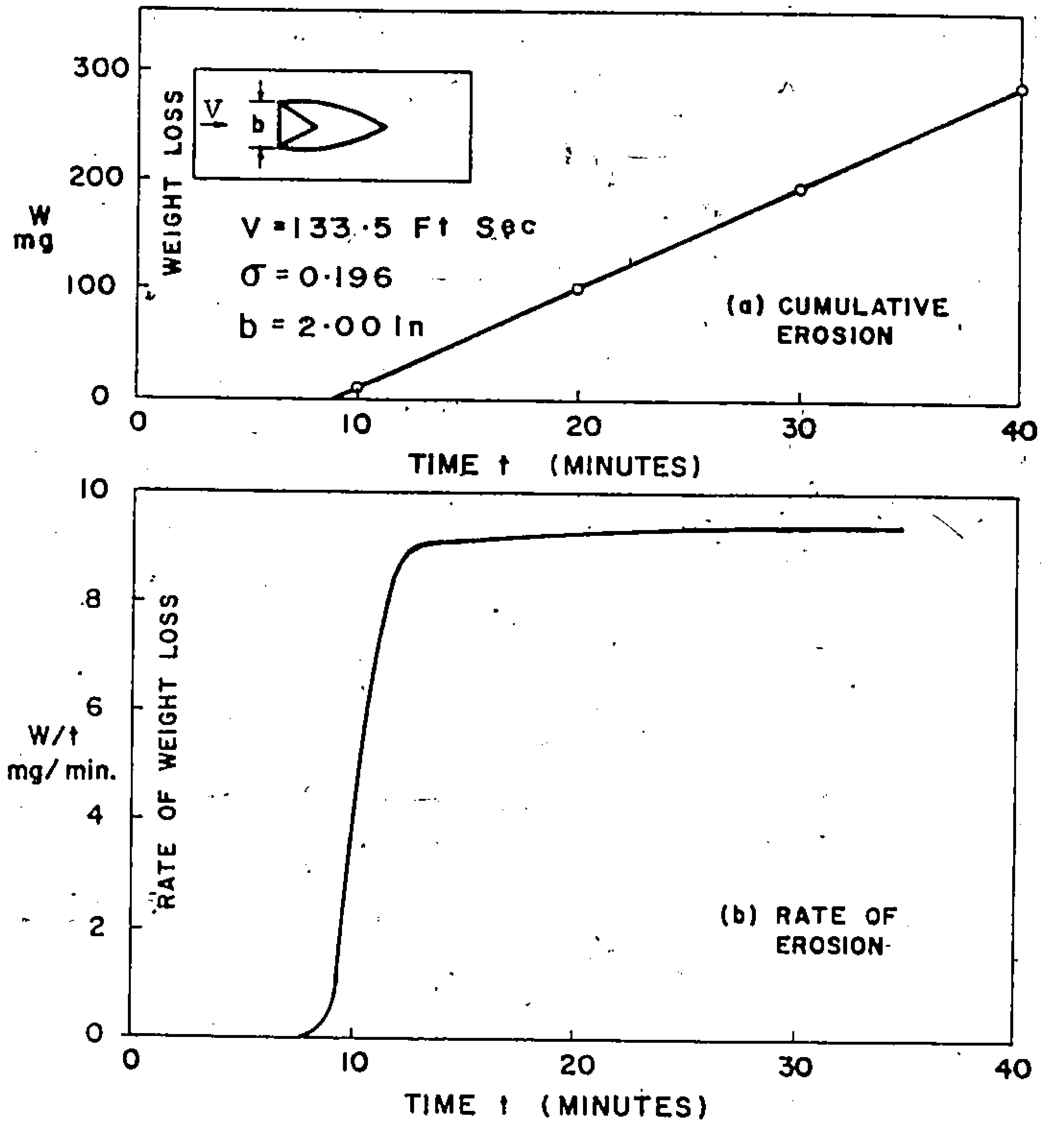

FIG. 3. EFFECT OF TEST DURATION ON DAMAGE ROTATING DISK APPARATUS

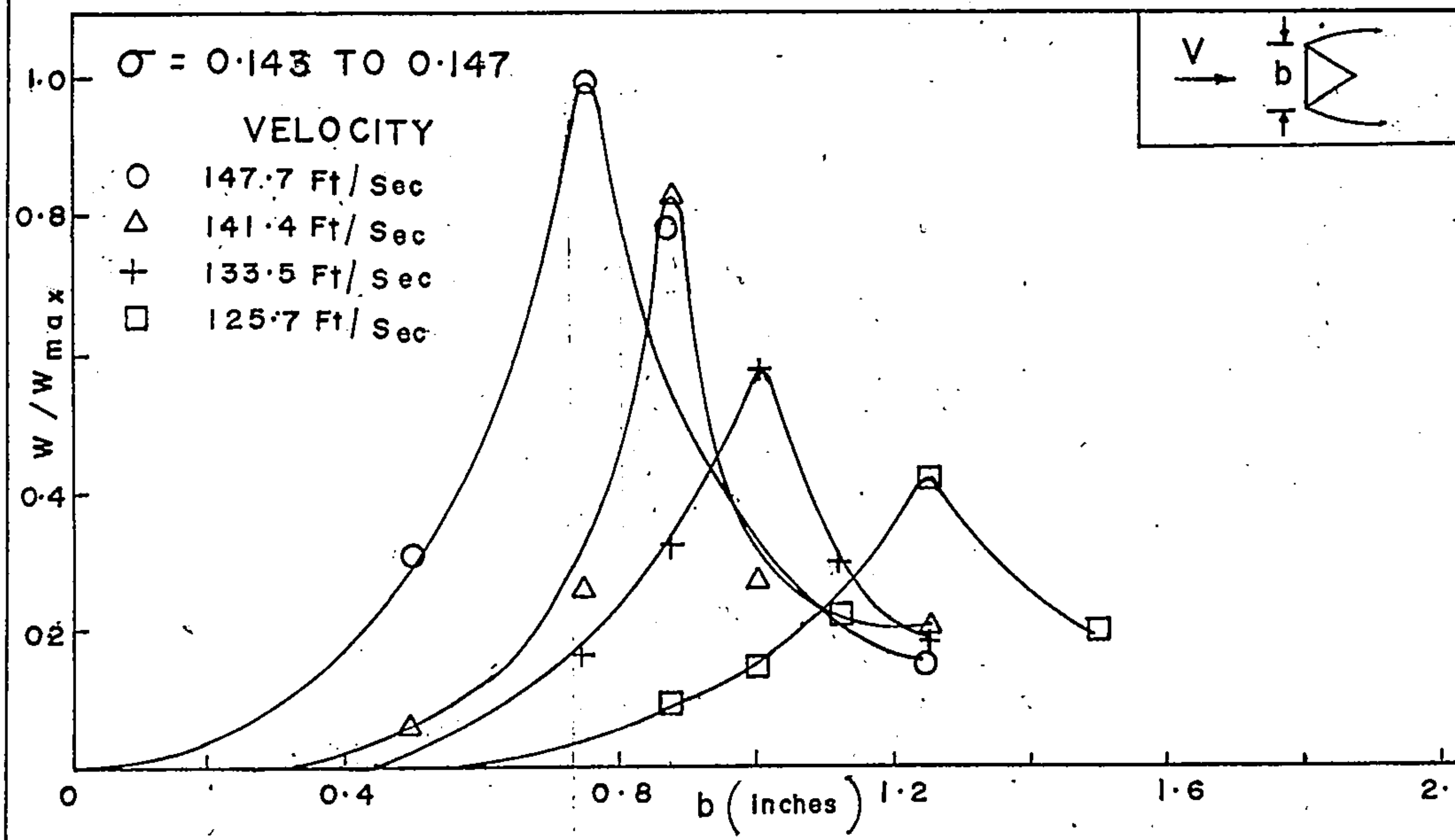

FIG. 4 EFFECT OF SOURCE SIZE ON CAVITATION DAMAGE

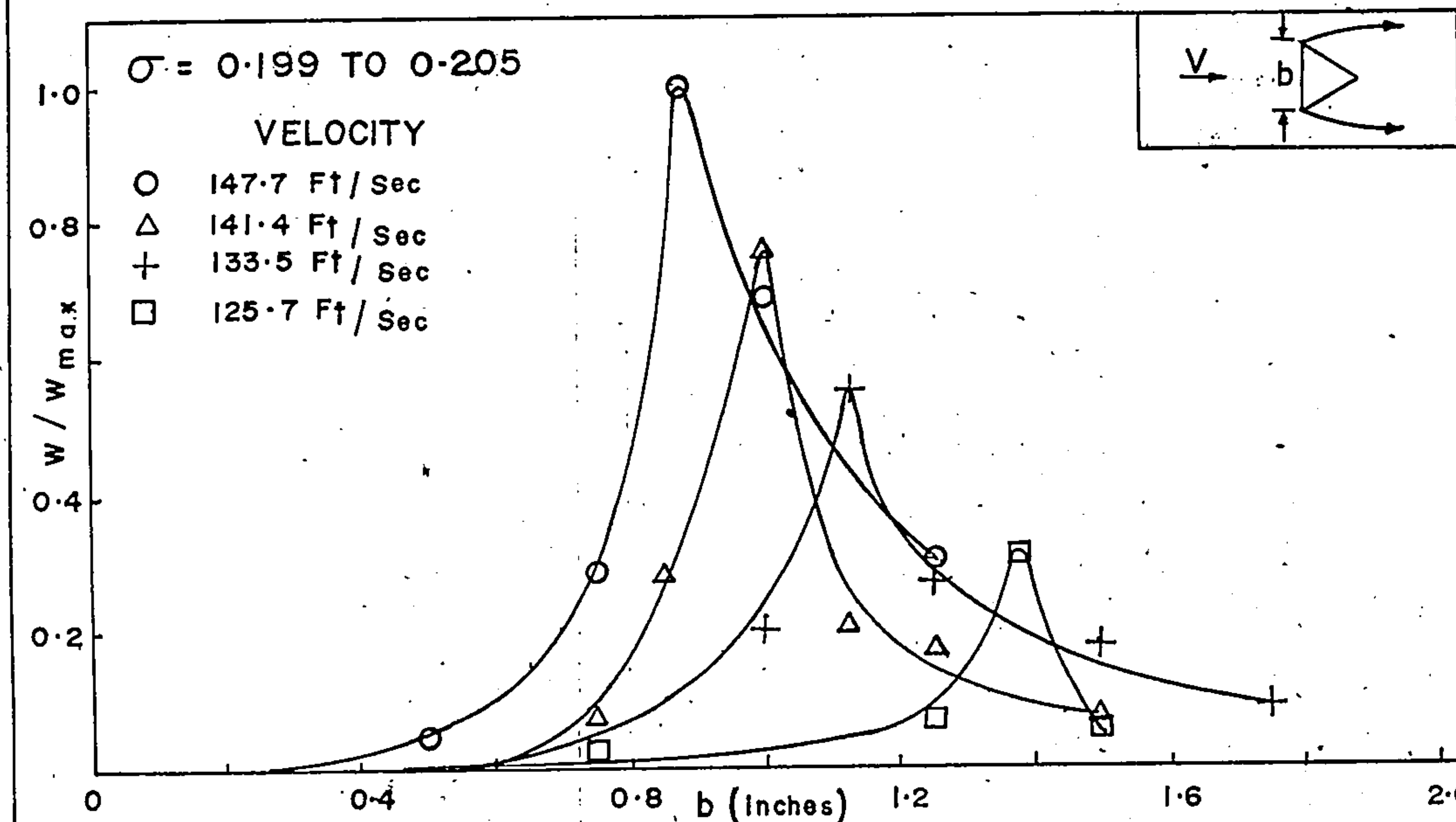

FIG. 5 EFFECT OF SOURCE SIZE ON CAVITATION DAMAGE

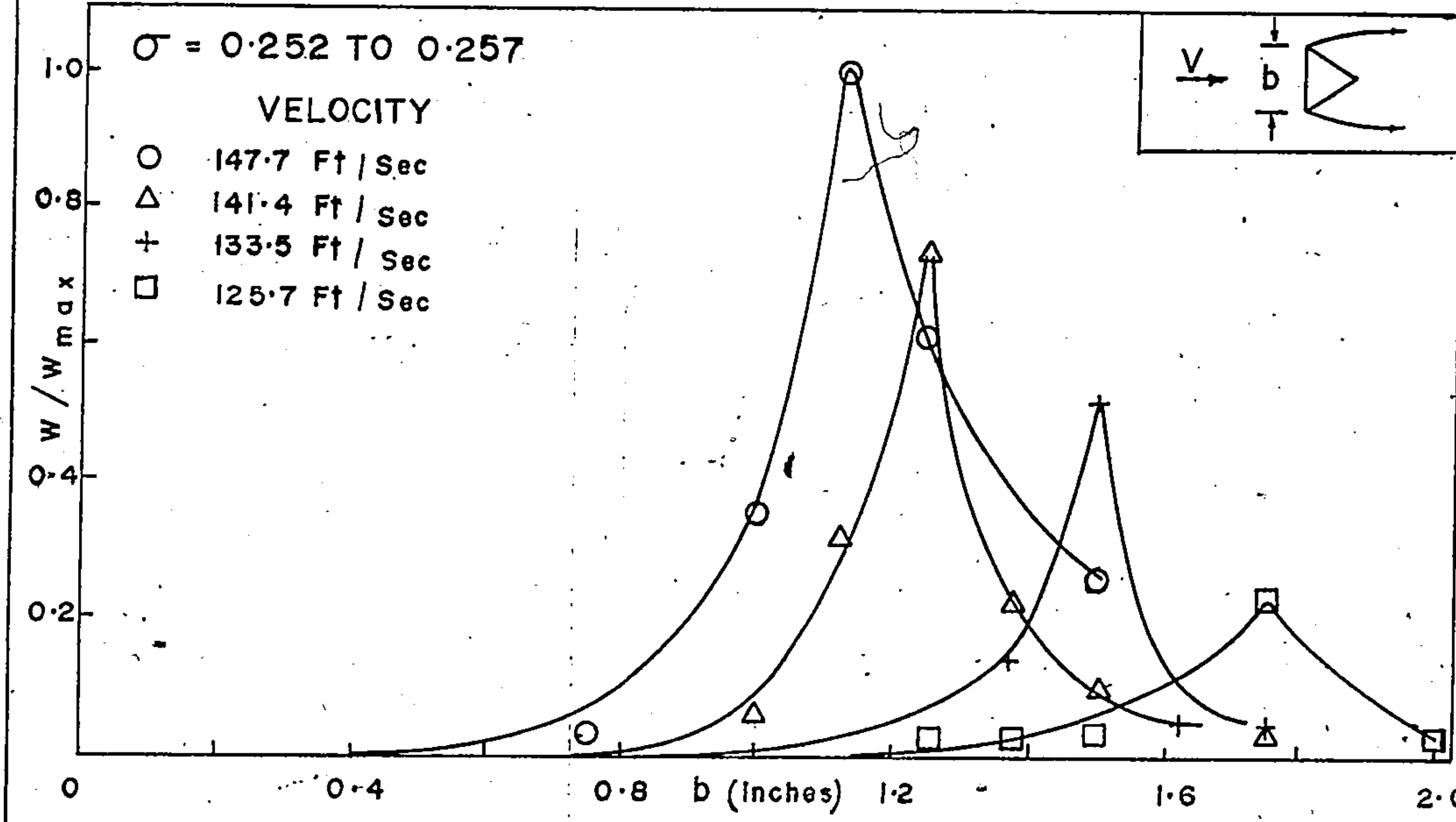

FIG. 6 EFFECT OF SOURCE SIZE ON CAVITATION DAMAGE

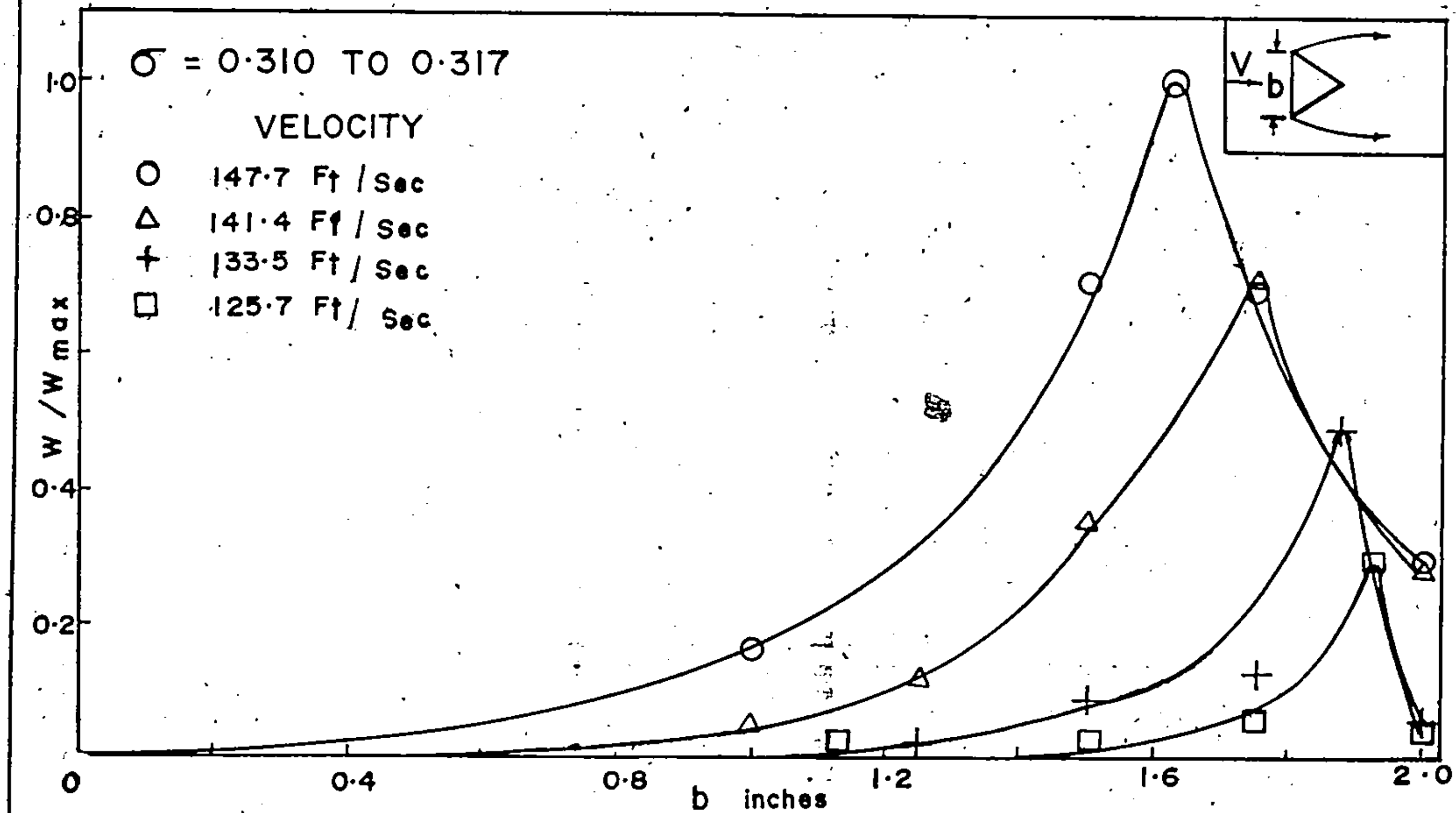

FIG. 7 EFFECT OF SOURCE SIZE ON CAVITATION DAMAGE

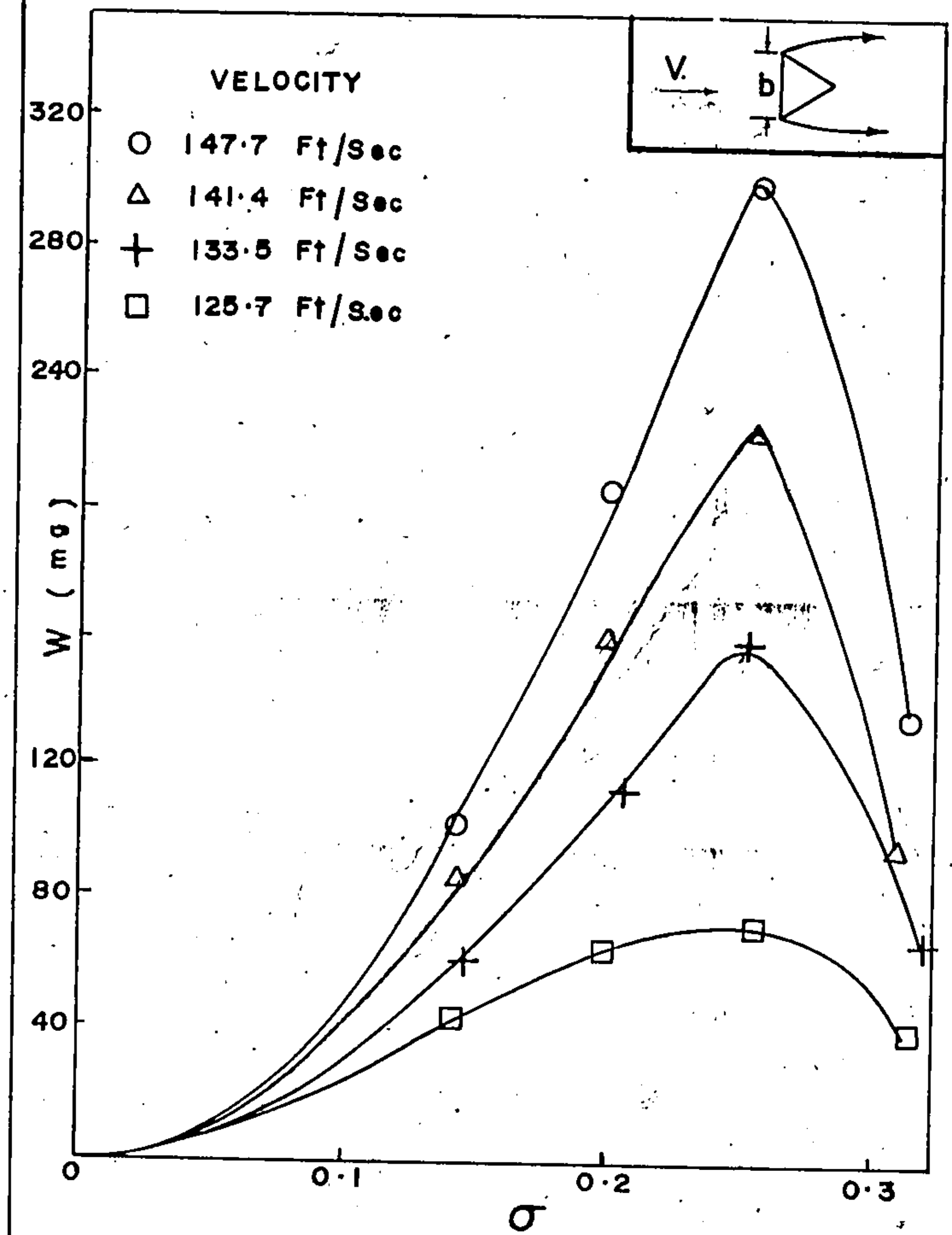

FIG. 8 EROSION FOR DIFFERENT VELOCITIES & CAVITATION NUMBERS

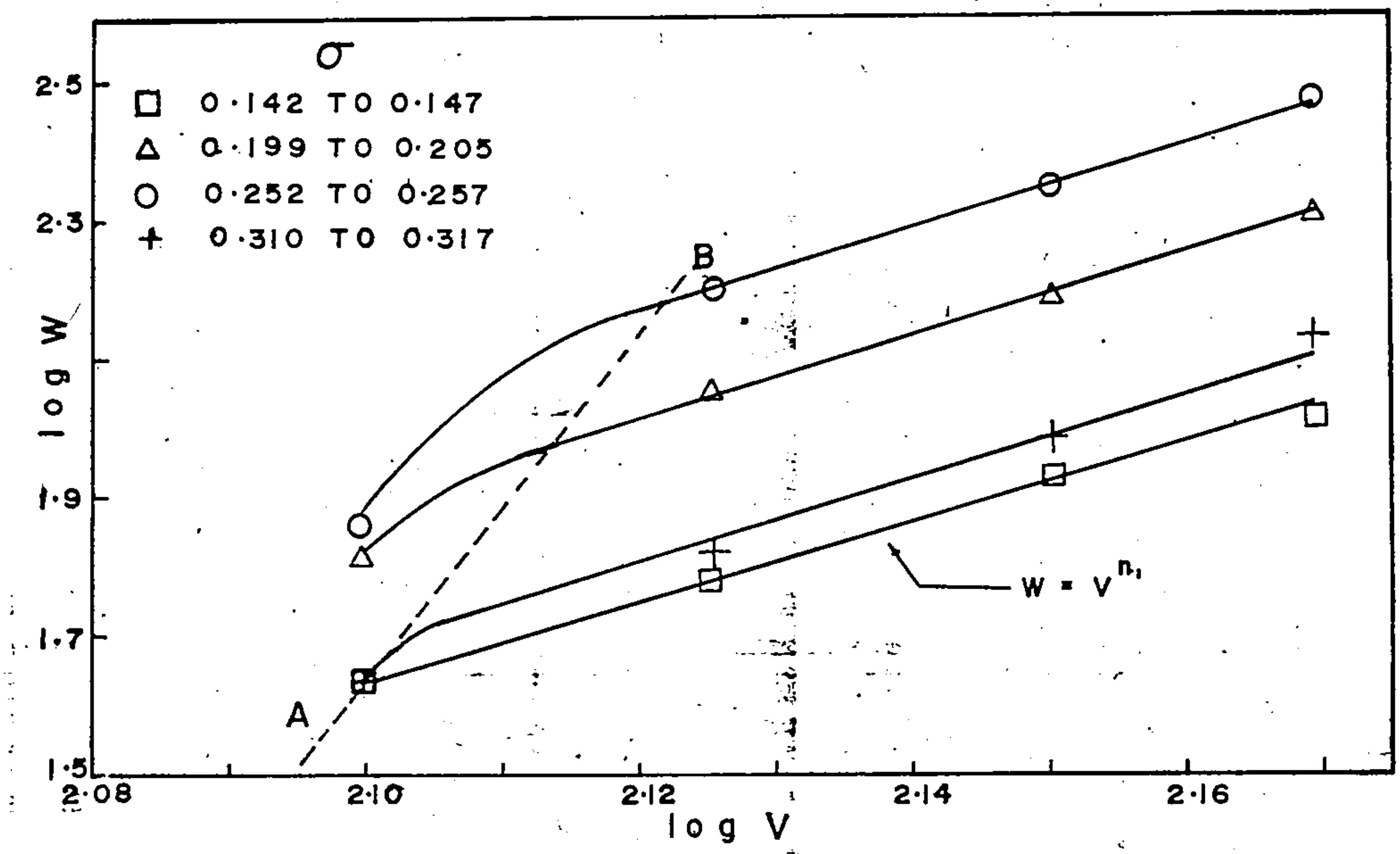

FIG. 9 VELOCITY EXPONENT FOR EROSION

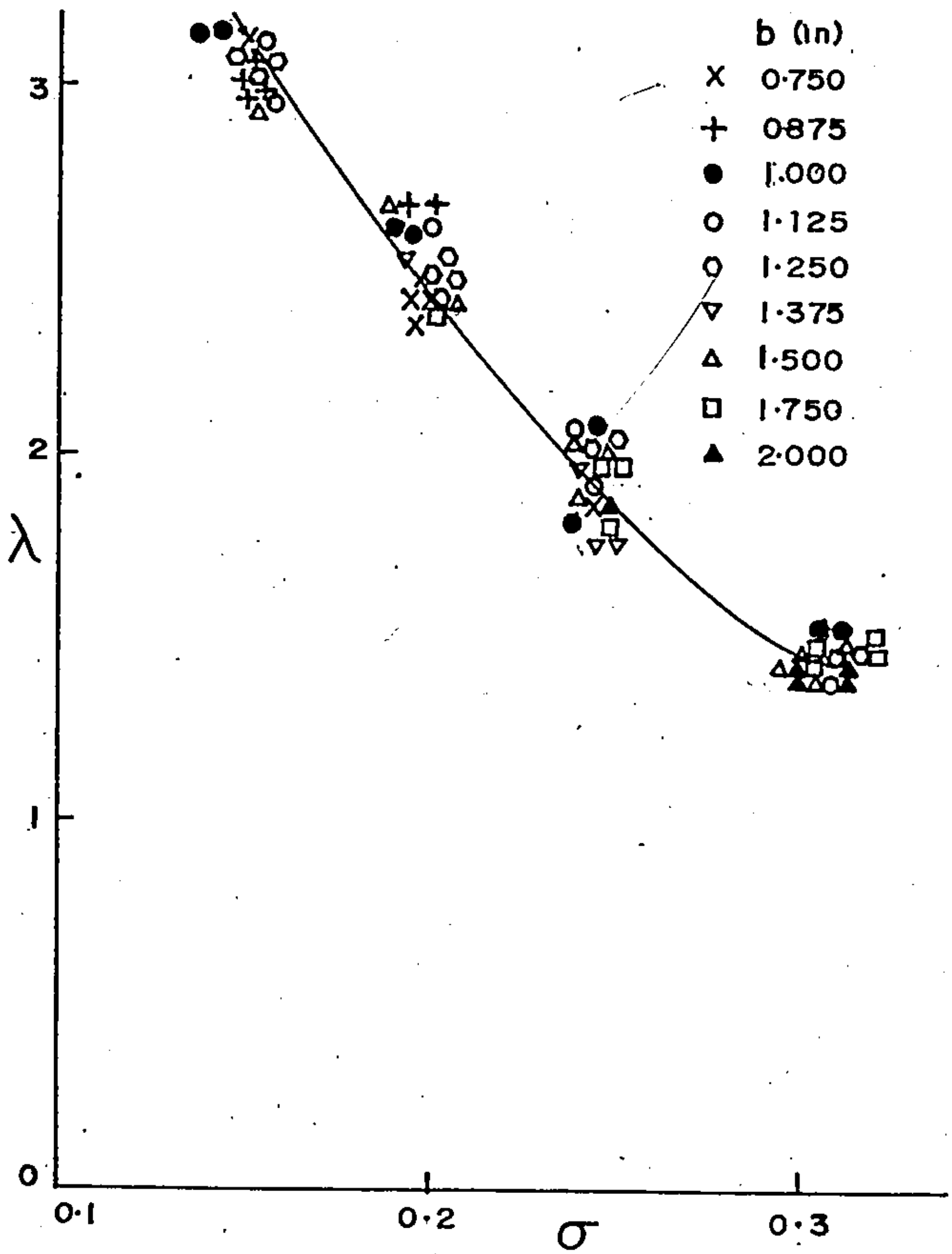

FIG· 10. NORMALISED CAVITY LENGTH AS A FUNCTION OF CAVITATION NUMBER

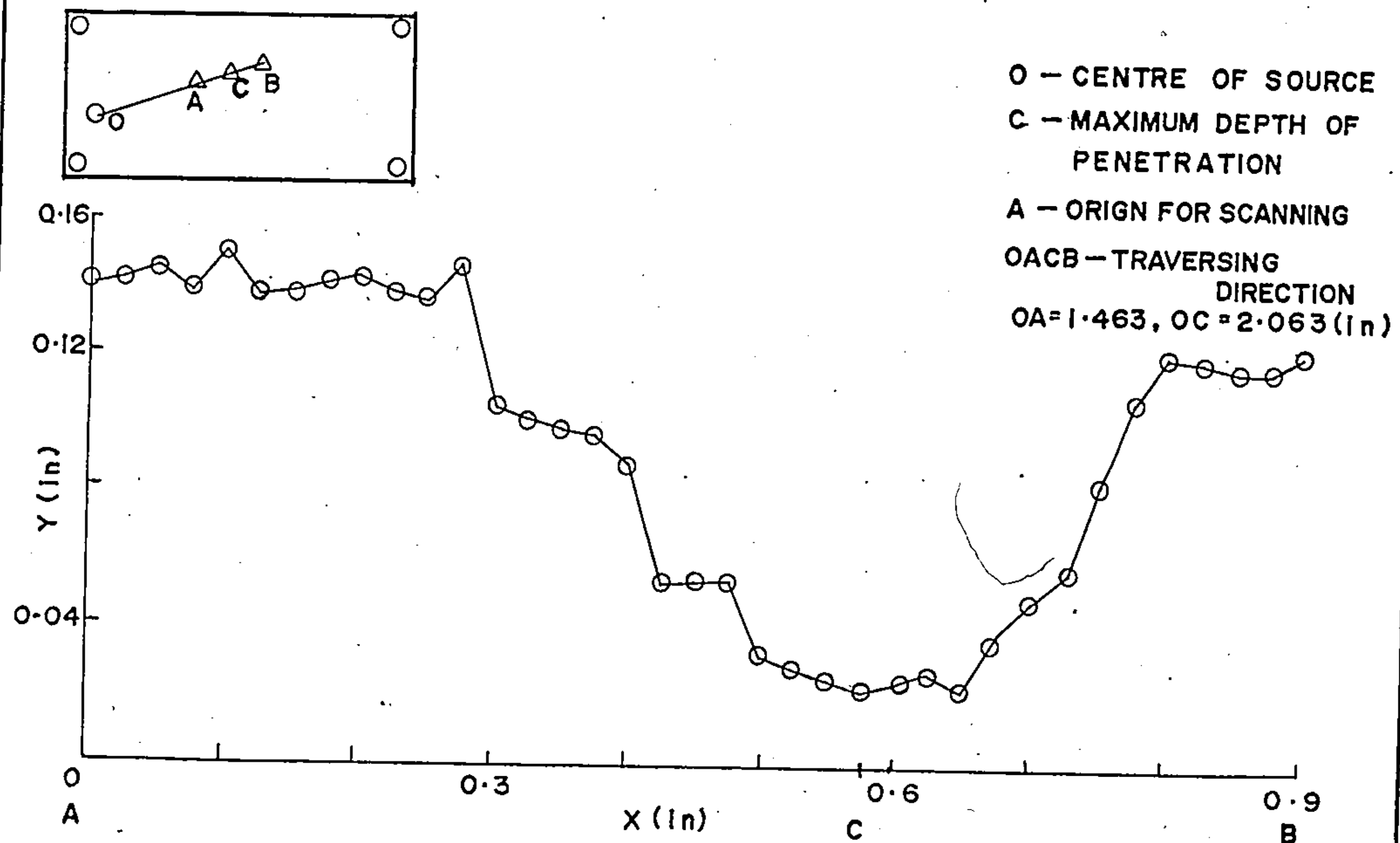

FIG. 11 SURFACE PROFILE OF THE DAMAGED SPECIMEN
(RUN 262, TABLE 4, P·46)

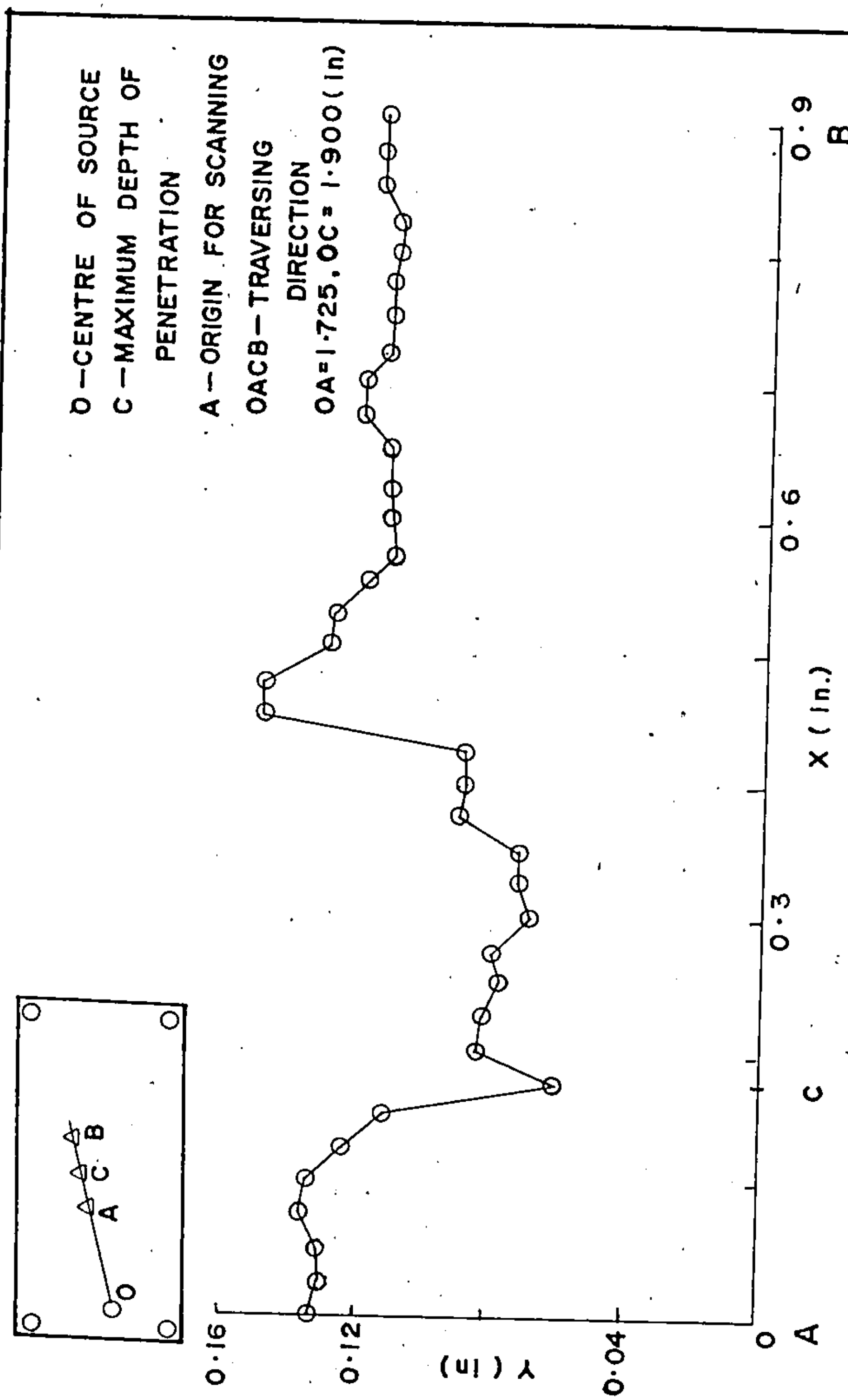

FIG 12 SURFACE PROFILE OF THE DAMAGED SPECIMEN
(RUN 128, TABLE 5, P·48)

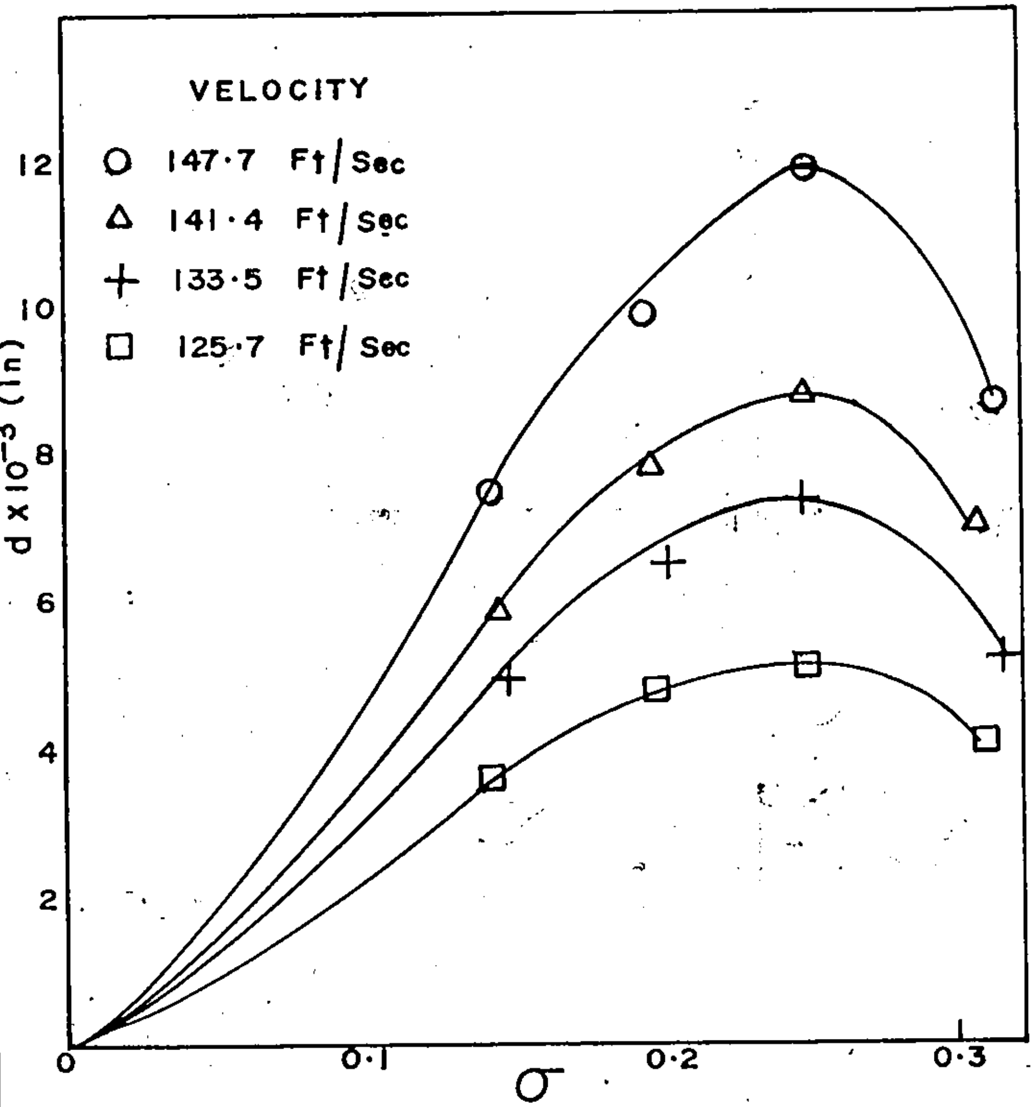

FIG·13 MAXIMUM DEPTH OF PENETRATION FOR DIFFERENT VELOCITIES & CAVITATION NUMBERS

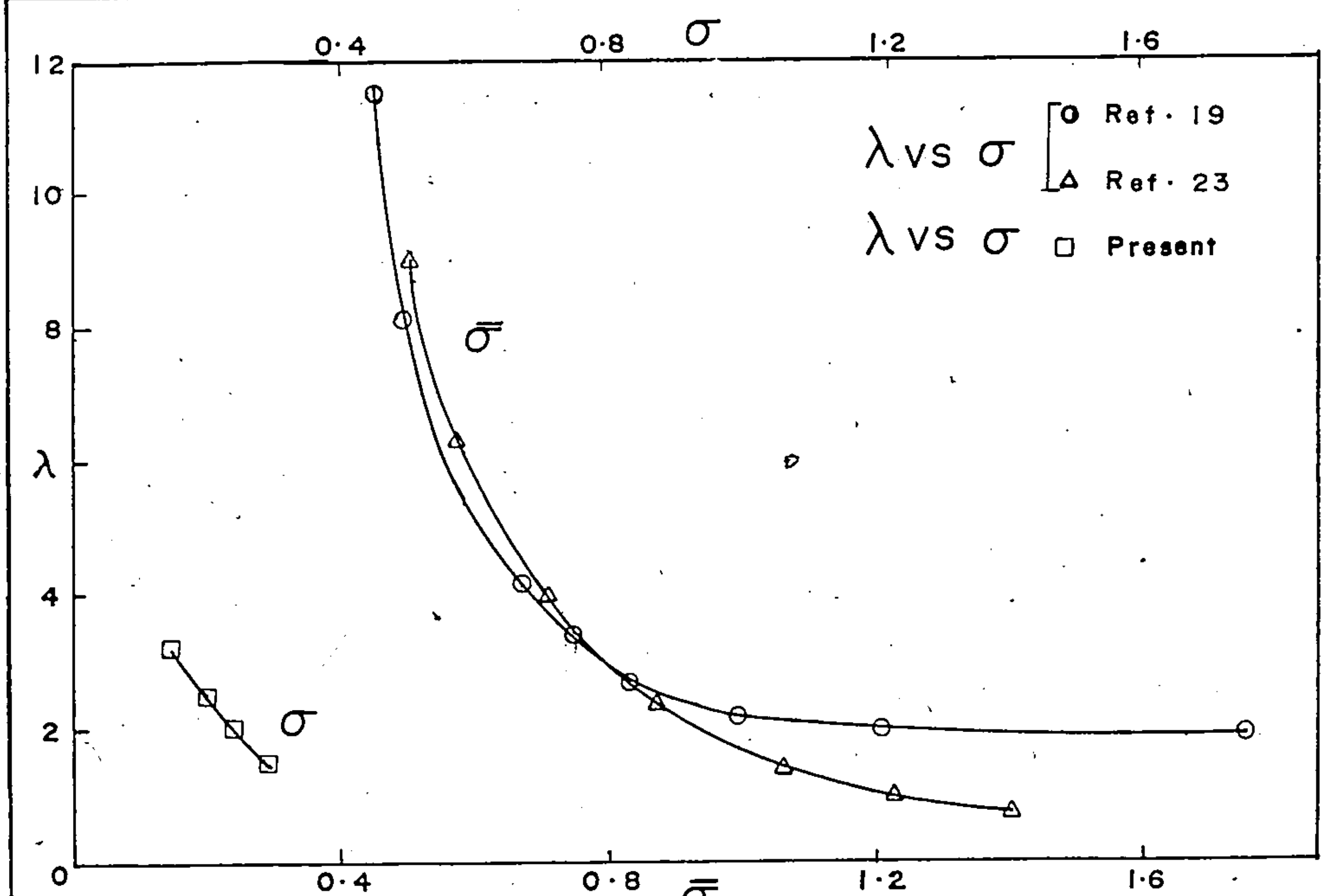

FIG·14 DIMENSIONLESS CAVITY LENGTH(λ) AS A FUNCTION OF CAVITATION NUMBER(σ) & MODIFIED CAVITATION NUMBER($\bar{\sigma}$) [AP·II]

TABLES

TABLE I SUMMARY OF DIFFERENT EXPERIMENTAL INVESTIGATIONS DETERMINING VELOCITY EXPONENT DUE TO CAVITATION EROSION

Type of Test Equipment	Material (Test Specimen)	Cavitation Number or Cavity Length	Test Duration	Velocity ft/sec	Erosion Criterion D	Velocity Exponent $D = KV^{n_1}$ $D = K(V-V_0)^{n_2}$
Axi-symmetric water tunnel, hemispherical nose ogival after body [12]	Aluminum 2S-F	l = 0.0082 in l = 0.167 in	10 min to 30 min	59 to 98	Number of pits per second per sq.in	$n_1 = 6$
Field test on 30,000 Kw Francis Turbine [13]	Aluminum 2S-0 test piece on runner	l = 0.499 to 0.666 in	5 min to 20 min	59 to 98	Number of pits per second per sq.in	$n_1 = 6$ (5.6'-6.3')
2-Dimensional water tunnel cylindrical source [16]	Lead	$\lambda = 3$ Near peak erosion	-----	46 to 75	Rate of volume erosion	n_1 = 4 to 5 Near peak erosion
Field hydraulic turbine [7]	Steel Runner	-----	up to 100 min	16 to 30	Radio isotope technique	n_1 = 5 to 8

Contd.

Type of Test Equipment	Material (Test Specimen)	Cavitation Number or Cavity Length	Test Duration	Velocity ft/sec	Erosion Criterion D	Velocity Exponent $D = KV^{n_1}$ $D = K(V-V_0)^{n_2}$
Venturi test rig cylindrical source [9]	Steel, Aluminum and plexiglass	Near peak erosion	varied	49 to 98	Volume loss	n_1 = 1.7 to 5. n_1 increases with test time
2-Dimensional water tunnel cylindrical source [24]	Lead	$\lambda = 3$	varied	30 to 46	Weight loss	n_1 = 2 to 5 n_1 increases with test time
Venturi test rig, tapered piece projecting into the venturi, mercury [8]	Stainless Steel 302	varied	30 to 100 hrs	20 to 66	Volume loss	$n_1 = \pm 1$ to 2
Venturi test rig, tapered piece projecting into the venturi, mercury [7]	Stainless Steel 302	varied	-----	20 to 66	Volume loss	n_1 = 0 to 5 dependent
2-Dimensional water tunnel, cylindrical source [17]	Lead	λ = 2.5 to 3	Incubation period	39 to 66	Volume loss	D and $L^3 V^{n_1}$ $n_1 = 5$

Contd.

Type of Test Equipment	Material (Test Specimen)	Cavitation Number or Cavity Length	Test Duration	Velocity ft/sec	Erosion Criterion D	Velocity Exponent $D = KV^{n_1}$ $D = K(V-V_0)^{n_2}$
Rotating disk in water, holes on the disk to induce cavitation [24]	8 different alloys	$\sigma = 0.084$ $\sigma = 0.1258$ $\sigma = 0.217$	up to 40 min	128 to 207	Volume loss	$1 < n_1 < 12$ $1 < n_2 < 7$ High exponent at low volume loss
Rotating disk cylindrical source [4]	Lead Antimony alloy	$\sigma = 0.25$ $\sigma = 0.50$ $\sigma = 0.75$	90 min	75 to 164	Weight loss	$7 < n_2 < 10$ $0.25 < \sigma < 0.75$ V_0 depends on static pressure
Rotating disk, equilateral prism - Apex facing downstream [14]	Aluminum 1100-F	$\sigma = 0.196$	30 min	138 to 151	Weight loss	$n_1 = 5.5$ for peak erosion and optimum source size
Rotating fail facility, hydrofoil (NACA-16-021) source [22]	Aluminum 1100-F	At peak erosion	10 to 70 hrs	161 to 194	Erosion intensity	$n_1 = 6$ Erosion depends on source size and σ.

TABLE 2: EXPERIMENTAL DATA - WEIGHT LOSS TESTS (σ = 0.143 to 0.147)

Ser. No.	Run No.	Velocity V(fps)	Pressure P(psi)	Cavitn. Number σ	Source Size b(in.)	Weight Loss W(mg.)	W/W_{max}	Cavity Length l(in.)	N.c.l λ	Temp. T(°F)	M.d.p d(in.)
1	271	147.7	21.500	0.143	0.500	32.0	0.3095	1.5750	3.1500	86	0.028
2	265	147.7	21.500	0.143	0.750	103.4	1.0000	2.3625	3.1500	86	0.075
3	270	147.7	21.500	0.143	0.875	80.5	0.7785	2.6250	3.0000	86	0.035
4	273	147.7	21.500	0.143	1.250	15.7	0.1518	3.9375	3.1500	86	0.019
5	149	141.4	20.325	0.147	0.500	6.2	0.0560	1.5750	3.1500	86	0.015
6	147	141.4	20.325	0.147	0.750	26.3	0.2544	2.3625	3.1500	86	0.041
7	210	141.4	20.325	0.147	0.875	86.3	0.8346	2.6250	3.0000	86	0.059
8	146	141.4	20.325	0.147	1.000	28.0	0.2708	3.1500	3.1500	86	0.035
9	150	141.4	20.325	0.147	1.250	20.7	0.2002	3.9375	3.1500	86	0.023
10	218	133.5	18.075	0.146	0.750	17.3	0.1673	2.3625	3.1500	86	0.023
11	219	133.5	18.075	0.146	0.875	33.0	0.3192	2.6250	3.0000	86	0.030

N.c.l Normalised Cavity Length.
M.d.p Maximum Depth of Penetration.

Contd.

TABLE 2: EXPERIMENTAL DATA - WEIGHT LOSS TESTS (σ = 0.143 to 0.147)

Ser. No.	Run No.	Velocity V(fps)	Pressure P(psi)	Cavitn. Number σ	Source Size b(in.)	Weight Loss W(mg.)	W/W_{max}	Cavity Length l(in.)	N.c.l λ	Temp. T(°F)	M.d.p d(in.)
12	216	133.5	18.075	0.146	1.000	60.0	0.5803	3.1500	3.1500	86	0.048
13	217	133.5	18.075	0.146	1.125	31.2	0.3017	3.4125	3.1500	85	0.026
14	220	133.5	18.075	0.146	1.250	20.2	0.1975	3.9375	3.1500	85	0.023
15	127	125.7	15.890	0.144	0.500	5.9	0.0571	1.5750	3.1500	86	0.009
16	049	125.7	15.890	0.144	0.875	9.7	0.0938	2.6250	3.0000	84	0.011
17	055	125.7	15.890	0.144	1.000	15.2	0.1470	3.1500	3.1500	85	0.017
18	124	125.7	15.890	0.144	1.125	24.0	0.2321	3.4125	3.0333	86	0.021
19	221	125.7	15.890	0.144	1.250	44.0	0.4255	3.9375	3.1500	86	0.036
20	211	125.7	15.890	0.144	1.500	20.5	0.1983	4.4625	2.9750	86	0.018
21	117	125.7	15.890	0.144	1.750	4.7	0.0455	4.7250	2.7000	85	0.006

N.c.l Normalised Cavity Length.
M.d.p Maximum Depth of Penetration.

TABLE 3: EXPERIMENTAL DATA - WEIGHT LOSS TESTS (σ = 0.199 to 0.205)

Ser. No.	Run No.	Veloc-ity V(fps)	Press-ure P(psi)	Cavitn. Number σ	Source Size b(in.)	Weight Loss W(mg.)	W/W_{max}	Cavity Length l(in.)	N.c.l λ	Temp. T(°F)	M.d.p d(in.)
1	286	147.7	29.790	0.199	0.500	9.1	0.0455	1.3125	2.6250	86	0.013
2	287	147.7	29.790	0.199	0.750	58.5	0.2861	1.8375	2.4500	86	0.039
3	263	147.7	29.790	0.199	0.875	204.5	1.0000	2.3625	2.7000	86	0.099
4	260	147.7	29.790	0.199	1.000	139.4	0.6817	2.6250	2.6250	86	0.037
5	285	147.7	29.790	0.199	1.250	62.5	0.3056	3.1500	2.5200	85	0.025
6	143	141.4	27.325	0.199	0.750	14.5	0.0709	1.8375	2.4500	86	0.012
7	145	141.4	27.325	0.199	0.875	57.8	0.2826	2.3625	2.7000	85	0.029
8	308	141.4	27.325	0.199	1.000	158.9	0.7526	2.6250	2.6250	86	0.078
9	144	141.4	27.325	0.199	1.125	42.6	0.2083	2.8875	2.5670	86	0.032
10	141	141.4	27.325	0.199	1.250	35.5	0.1736	3.1500	2.5200	86	0.019
11	140	141.4	27.325	0.199	1.500	15.5	0.0758	3.9375	2.6250	86	0.018

N.c.l Normalised Cavity Length.
M.d.p Maximum Depth of Penetration.

Contd.

TABLE 3: EXPERIMENTAL DATA - WEIGHT LOSS TESTS (σ = 0.199 to 0.205)

Ser. No.	Run No.	Velocity V(fps)	Pressure P(psi)	Cavitn. Number σ	Source Size b(in.)	Weight Loss W(mg.)	W/W_{max}	Cavity Length l(in.)	N.c.l λ	Temp. T(°F)	M.d.p d(in.)
12	038	133.5	24.925	0.205	0.750	7.5	0.0367	2.1000	2.5000	86	0.012
13	298	133.5	24.925	0.205	1.000	41.4	0.2025	2.1000	2.8000	85	0.023
14	307	133.5	24.925	0.205	1.125	112.2	0.5487	2.6250	2.5670	86	0.065
15	296	133.5	24.925	0.205	1.250	55.7	0.2724	2.8875	2.5200	85	0.043
16	300	133.5	24.925	0.205	1.500	36.0	0.1760	3.1500	2.4500	86	0.032
17	039	133.5	24.925	0.205	1.750	17.9	0.0875	3.6750	2.4000	85	0.012
18	303	125.7	21.720	0.199	0.750	5.0	0.0245	2.1000	2.5000	85	0.006
19	280	125.7	21.720	0.199	1.250	13.2	0.0646	3.1500	2.5200	85	0.022
20	301	125.7	21.720	0.199	1.375	65.1	0.3183	3.4125	2.4820	86	0.047
21	277	125.7	21.720	0.199	1.500	10.4	0.0509	3.6750	2.4500	86	0.008

N.c.l Normalised Cavity Length.
M.d.p Maximum Depth of Penetration.

TABLE 4 EXPERIMENTAL DATA - WEIGHT LOSS TESTS (σ = 0.252 to 0.257)

Ser. No.	Run No.	Velocity V(fps)	Pressure P(psi)	Cavitn. Number σ	Source Size b(in.)	Weight Loss W(mg.)	W/W_{max}	Cavity Length l(in.)	N.c.l λ	Temp. T(°F)	M.d.p d(in.)
1	283	147.7	38.140	0.256	0.750	9.9	0.0329	1.5750	2.1000	85	0.005
2	284	147.7	38.140	0.256	1.000	106.5	0.3535	2.1000	2.1000	86	0.052
3	262	147.7	38.140	0.256	1.125	301.3	1.0000	2.1000	1.8670	86	0.118
4	261	147.7	38.140	0.256	1.250	184.7	0.6130	2.6250	2.1000	87	0.098
5	281	147.7	38.140	0.256	1.500	78.5	0.2605	2.6250	1.7500	86	0.081
6	136	141.4	34.450	0.252	1.000	19.0	0.0631	1.8375	1.8375	85	0.018
7	138	141.4	34.450	0.252	1.125	96.3	0.3196	2.3625	2.1000	86	0.026
8	310	141.4	34.450	0.252	1.250	223.4	0.7415	2.6250	2.1000	86	0.089
9	137	141.4	34.450	0.252	1.375	68.5	0.2274	2.3625	1.7182	86	0.029
10	134	141.4	34.450	0.252	1.500	32.1	0.1065	2.8875	1.9250	86	0.019
11	133	141.4	34.450	0.252	1.750	9.7	0.0327	3.4125	1.9500	86	0.009

N.c.l Normalised Cavity Length.
M.d.p Maximum Depth of Penetration.

Contd.

TABLE 4: EXPERIMENTAL DATA - WEIGHT LOSS TESTS (σ = 0.252 to 0.257)

Ser. No.	Run No.	Velocity V(fps)	Pressure P(psi)	Cavitn. Number σ	Source Size b(in.)	Weight Loss W(mg.)	W/W_{max}	Cavity Length l(in.)	N.c.l λ	Temp. T(°F)	M.d.p d(in.)
12	291	133.5	30.950	0.252	1.375	42.8	0.1412	2.6250	1.9091	86	0.017
13	293	133.5	30.950	0.252	1.500	158.6	0.5264	2.8875	1.9250	86	0.074
14	292	133.5	30.950	0.252	1.625	16.0	0.0531	3.1500	1.9385	86	0.031
15	295	133.5	30.950	0.252	1.750	13.5	0.0448	3.4125	1.9500	86	0.013
16	110	125.7	27.850	0.257	1.250	4.8	0.0159	2.6250	2.1000	85	0.003
17	111	125.7	27.850	0.257	1.375	8.2	0.0272	2.3625	1.7182	85	0.016
18	109	125.7	27.850	0.257	1.500	10.3	0.0342	2.8875	1.9250	85	0.021
19	278	125.7	27.850	0.257	1.625	15.4	0.0511	3.1500	1.9385	86	0.030
20	279	125.7	27.850	0.257	1.750	72.1	0.2393	3.1500	1.8000	86	0.051
21	302	125.7	27.850	0.257	2.000	10.1	0.0375	3.6750	1.8375	86	0.010

N.c.l Normalised Cavity Length.
M.d.p Maximum Depth of Penetration.

TABLE 5: EXPERIMENTAL DATA - WEIGHT LOSS TESTS (σ = 0.310 to 0.317)

Ser. No.	Run No.	Velocity V(fps)	Pressure P(psi)	Cavitn. Number σ	Source Size b(in.)	Weight Loss W(mg.)	W/W_{max}	Cavity Length l(in.)	N.c.l λ	Temp. T(°F)	M.d.p d(in.)
1	288	147.7	46.700	0.315	1.000	21.8	0.1608	1.5750	1.5750	86	0.031
2	282	147.7	46.740	0.315	1.500	96.2	0.7094	2.100	1.4000	85	0.067
3	272	147.7	46.740	0.315	1.625	135.6	1.0000	2.3625	1.4539	86	0.086
4	264	147.7	46.740	0.315	1.750	94.1	0.6940	2.6750	1.5000	86	0.076
5	289	147.7	46.740	0.315	2.000	40.0	0.2950	2.8875	1.4438	85	0.068
6	130	141.4	42.200	0.310	1.000	7.3	0.0538	1.5750	1.5750	86	0.009
7	193	141.4	42.200	0.310	1.250	10.3	0.1202	1.8375	1.4700	85	0.014
8	131	141.4	42.200	0.310	1.500	48.6	0.3584	2.1000	1.4000	86	0.032
9	128	141.4	42.200	0.310	1.750	96.4	0.7109	2.6250	1.5000	86	0.069
10	132	141.4	42.200	0.310	2.000	38.8	0.2861	2.8875	1.4438	86	0.012
11	030	133.5	38.450	0.317	1.250	3.2	0.0236	1.8375	1.4700	86	0.009

N.c.l Normalised Cavity Length.
M.d.p Maximum Depth of Penetration.

Contd.

TABLE 5 : EXPERIMENTAL DATA - WEIGHT LOSS TESTS (σ = 0.310 to 0.317)

Ser. No.	Run No.	Velocity V(fps)	Pressure P(psi)	Cavitn. Number σ	Source Size b(in.)	Weight Loss W(mg.)	W/W_{max}	Cavity Length l(in.)	N.c.l λ	Temp. T(°F)	M.d.p d(in.)
12	231	133.5	38.450	0.317	1.500	11.4	0.0841	2.1000	1.4000	86	0.013
13	031	133.5	38.450	0.317	1.750	16.5	0.1217	2.6250	1.5000	86	0.018
14	239	133.5	38.450	0.317	1.875	66.4	0.4897	2.6250	1.4000	86	0.051
15	233	133.5	38.450	0.317	2.000	8.9	0.0656	2.8875	1.4438	86	0.011
16	108	125.7	33.575	0.311	1.125	2.8	0.0207	1.5750	1.4000	85	0.002
17	118	125.7	33.575	0.311	1.500	3.9	0.0288	2.1000	1.4000	87	0.005
18	305	125.7	33.575	0.311	1.750	7.6	0.0561	2.6250	1.5000	85	0.016
19	238	125.7	33.575	0.311	1.925	40.9	0.3016	2.6250	1.3636	86	0.041
20	304	125.7	33.575	0.311	2.000	5.5	0.0406	2.8875	1.4438	86	0.007

N.c.l Normalised Cavity Length.
M.d.p Maximum Depth of Penetration.

TABLE 6: COMPUTATION OF VELOCITY EXPONENT

Ser. No.	Run No.	Weight Loss W(mg.)	$\log_{10}W$	Velocity V(fps)	$\log_{10}V$	Source Size b(in.)	Cavitn. Number σ
1	272	135.6	2.1323	147.7	2.1694	1.625	0.315
2	128	96.4	1.9841	141.4	2.1501	1.750	0.310
3	239	66.4	1.8222	133.5	2.1255	1.875	0.317
4	238	40.9	1.6117	125.7	2.0993	1.925	0.311
5	262	301.3	2.4790	147.7	2.1694	1.125	0.256
6	310	223.4	2.3491	141.4	2.1501	1.250	0.252
7	293	158.6	2.2003	133.5	2.1255	1.500	0.252
8	279	72.1	1.8579	125.7	2.0993	1.625	0.257
9	263	204.5	2.3107	147.7	2.1694	0.875	0.199
10	308	158.9	2.2011	141.4	2.1501	1.000	0.199
11	307	112.2	2.0500	133.5	2.1255	1.125	0.205
12	301	65.1	1.8136	125.7	2.0993	1.375	0.199
13	265	103.4	2.0145	147.7	2.1694	0.750	0.143
14	210	86.3	1.9360	141.4	2.1501	0.875	0.147
15	216	60.0	1.7782	133.5	2.1255	1.000	0.146
16	221	44.0	1.6435	125.7	2.0993	1.250	0.144

APPENDIX I

SPECIMEN COMPUTATIONS

SPECIMEN COMPUTATIONS

A1.1 COMPUTATION OF CAVITATION NUMBER

Computation refers to RUN 263 of Table III.

Radius (r) = 0.783 ft

Angular velocity (n) = 1,800 RPM

Circumferential velocity (v) = $\frac{2\pi r \Omega n}{60}$

$= \frac{2 \times \pi \times 0.783 \times 1,800}{60} = 147.7$ ft/sec.

$P_{absolute} = P_{gauge} + P_{atmospheric}$

= 15.09 + 14.7 = 29.79 psi

At 86°F,

$P_V = 0.6216$ psi

$\rho = 1.932$ slugs/ft^3

$v = 147.7$ ft/sec

$\sigma = [(P-P_V)/(\frac{1}{2}\ \rho\ V^2)] \times 144$

$= [(29.79-0.6216)/(\frac{1}{2} \times 1.932 \times 147.7^2)]$

$\times 144 = 0.199$

A1.2 COMPUTATION OF VELOCITY EXPONENT

Weight loss,

$$W \propto V^{n_1}$$

or

$$\log_{10} W \propto n_1 \log_{10} V$$

At maximum erosion conditions, from Figure 9, the slope of the line $\log_{10} W$ versus $\log_{10} V$ gives

$$n_1 = 5.95$$

APPENDIX II

CAVITY LENGTH CHARACTERISTICS

APPENDIX II

CAVITY LENGTH CHARACTERISTICS

Considerable studies have been made to relate the length of the cavity with cavitation numbers [19,23]. Varga [23] has shown a relation of the form

$$\lambda\, [\bar{\sigma}]^{n} = \text{const} \qquad \text{(A2.1)}$$

holds good for flow past a cavitating cylindrical source, set in a venturi flow apparatus. In the above equation $\bar{\sigma}$ is the cavitation number based on contracted jet velocity and λ is the normalised cavity length.

Syamala Rao and Chandrashekara [19] have confirmed the existence of a relation similar to that of Equation A2.1 . It may be added that Birkoff [3b] has indicated that one could use the contracted jet velocity u_j as the normalising velocity scale when blockage effects are present. Blockage denotes the interference caused by the side walls of the water tunnel on the flow past an oversized model. Figure 13 shows the variation of λ with σ [19,23].

For the case of flow past triangular prisms, the variation of the normalised cavity length with cavitation number, from the present tests, is shown in Fig. 14. It is seen that the flow past a triangular prism mounted on a rotating disk is highly sheared and it is difficult to make comparison of the present data (Fig. 14) with the results of earlier investigators (Fig. 13).

The variation of normalised cavity length with cavitation number appears to be independent of the source size for the data obtained. In other words, one could conveniently adapt the normalised cavity length as a parameter in the place of the cavitation number while studying the cavitation erosion characteristics.

APPENDIX III

SURFACE CHARACTERISTICS OF THE TEST SPECIMEN

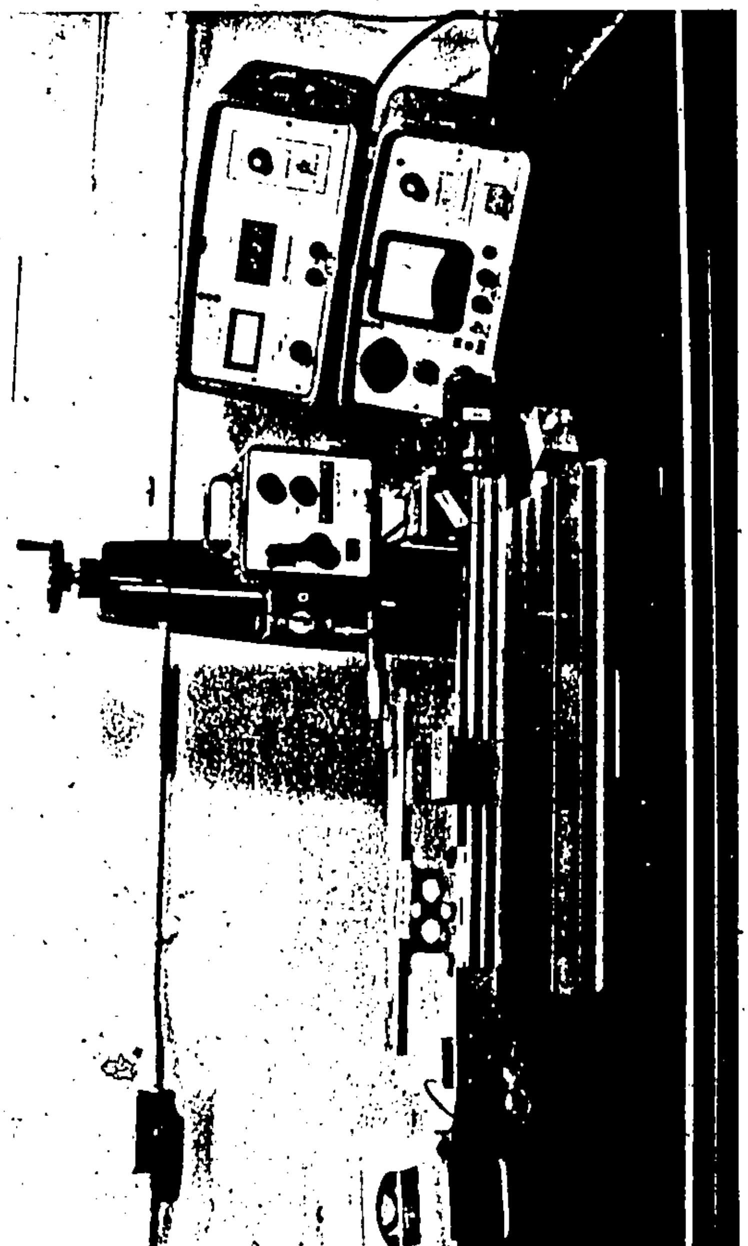

PLATE. I TELESURF

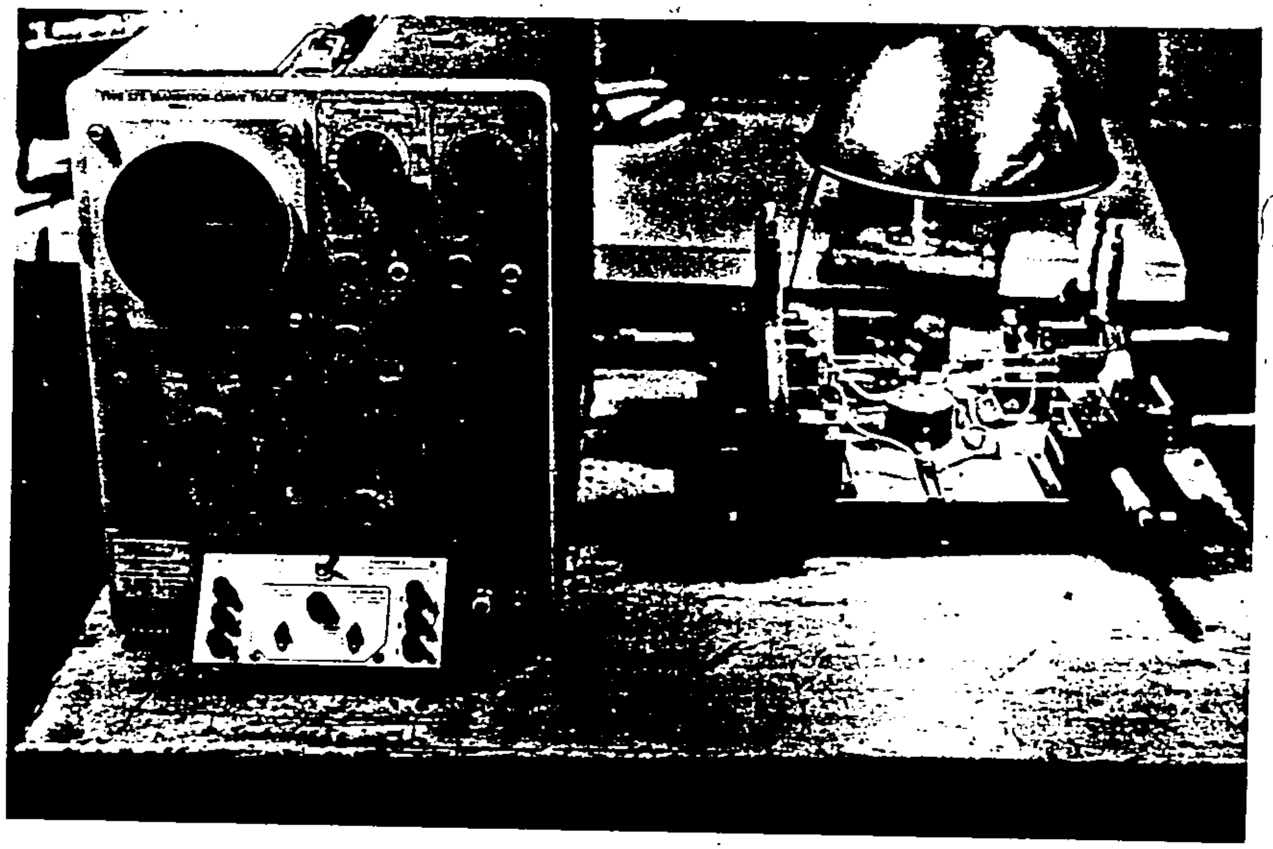

PLATE. 2 MICRO-POSITIONER

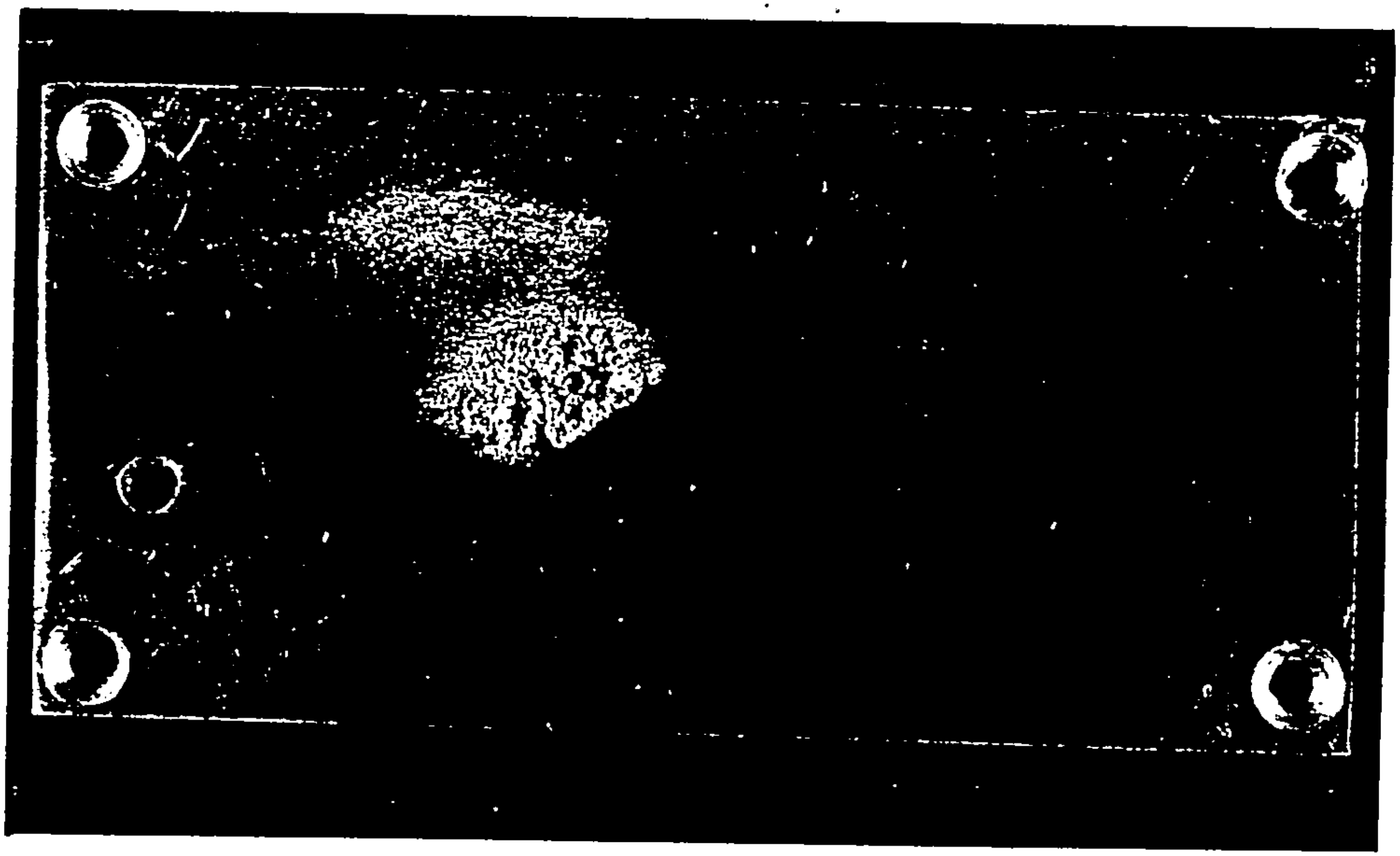

PLATE.3 DAMAGED AREA OF TEST SPECIMEN (RUN 262, TABLE 4 P.46)

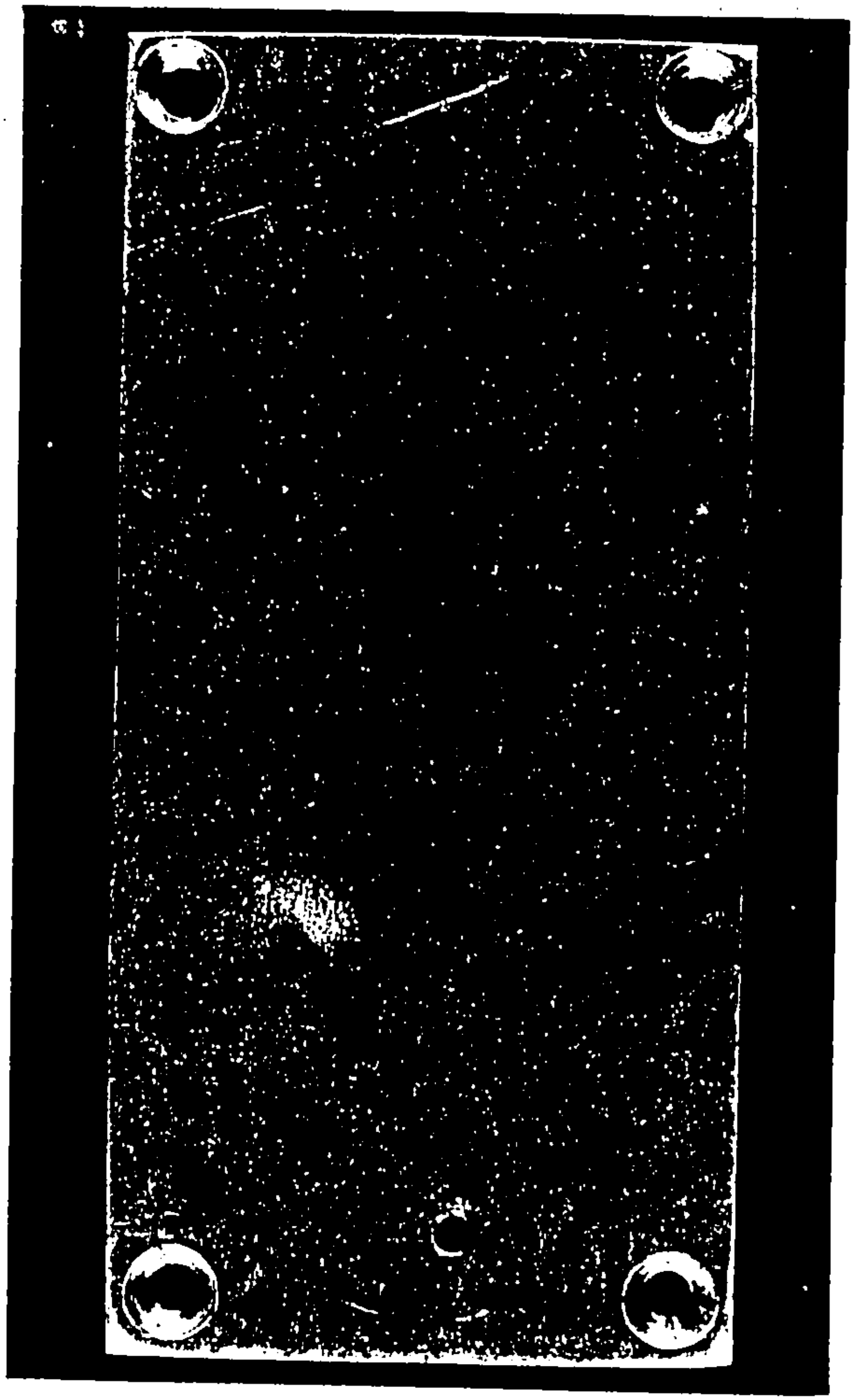

PLATE.4 DAMAGED AREA OF TEST SPECIMEN(RUN 211, TABLE 2, P.43)

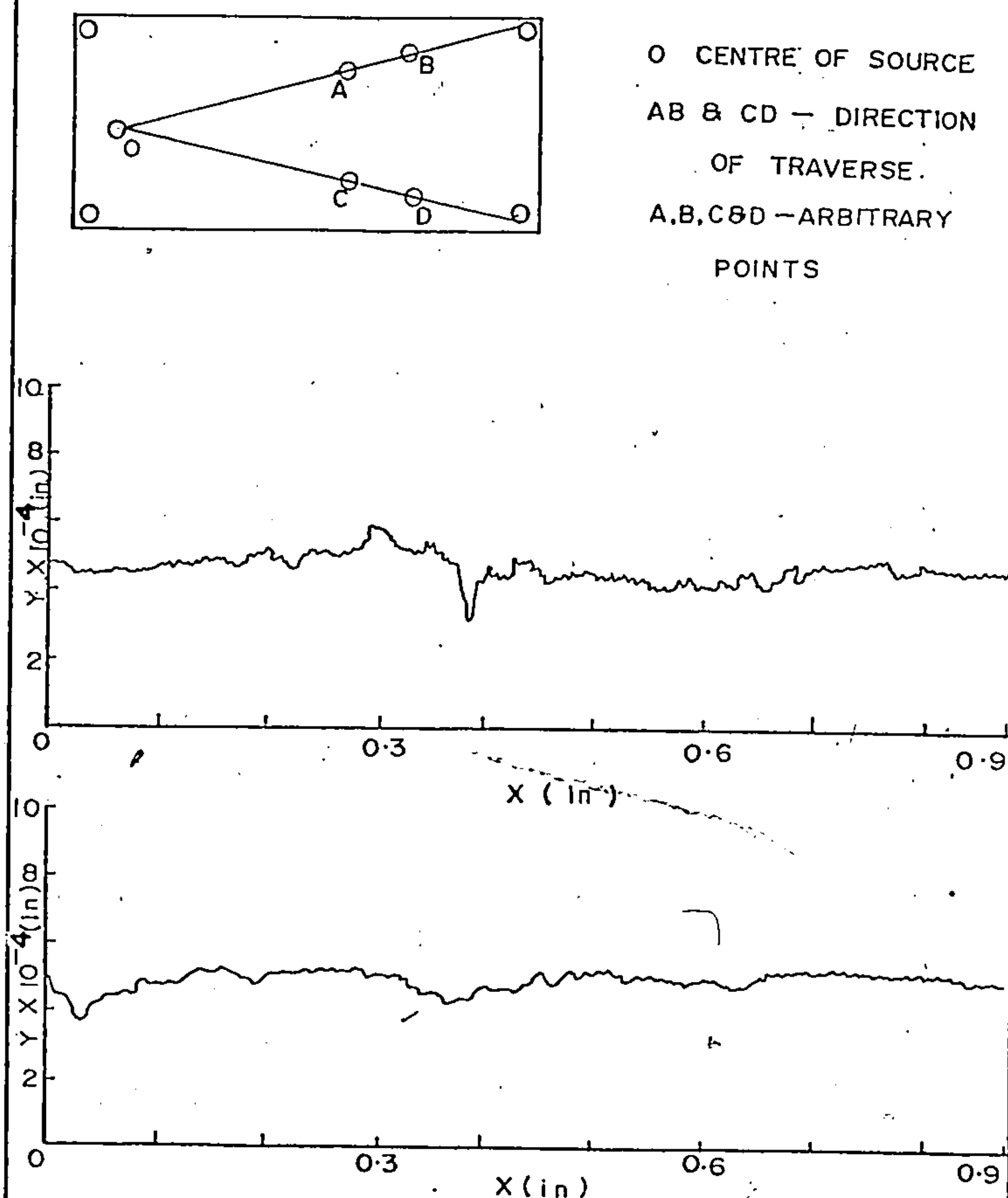

FIG. A1, TYPICAL SURFACE PROFILE OF THE SPECIMEN BEFORE THE TEST

APPENDIX IV

EXPERIMENTAL ERRORS

EXPERIMENTAL ERRORS

FIGURE	TITLE	REMARKS - ERROR RANGE
1	Rotating disk facility	---
2	Source shape and size	Linear measurement ± 0.001" Angular measurement ± 30"
3	Effect of test duration on damage	Time ± 1 sec. Weight loss: ± 0.5 mg ν ± 0.05 fps σ ± 0.001
4	Effect of source size on cavitation damage	b ± 0.001" v ± 0.05 fps w ± 0.05 mg t ± 1 second σ ± 0.001
5	Effect of source size on cavitation damage	as in Fig. 4
6	Effect of source size on cavitation damage	as in Fig. 4

FIGURE	TITLE	REMARKS - ERROR RANGE
7	Effect of source size on cavitation damage	as in Fig. 4
8	Erosion for different velocities and cavitation numbers	time ± 1 second V ± 0.05 fps W ± 0.005 mg σ ± 0.001
9	Velocity exponent for Erosion	weight loss ± 0.05mg
10	Normalised cavity length as a function of cavitation number	linear measurement ±0.001" σ± 0.001
11	Surface profile of the damaged specimen	linear measurement ±0.001"
12	Surface profile of the damaged specimen	as in fig.11
13	Maximum depth of penetration for different velocities and cavitation numbers	linear measurements ±0.001" σ± 0.001
14	Dimensionless cavity length as a function of cavitation number and modified cavitation number	--------
15	Typical surface profile of the specimen before the test	linear measurements ±0.0004"